

Liverpool Project, Arnhem Land, NT Argus™ / Magnetic / Spectrometer Geophysical Survey

Acquisition and Processing Report for



Cameco Australia Pty Ltd

A.C.N. 001 513 088

Prepared by : P.Chambers

S.Baron-Hay

L.Stenning

Authorised for release by :

.....

Survey flown: October 2000 – January 2001

by



Fugro Airborne Surveys

65 Brockway Road, Floreat. WA 6014, Australia

Tel: (61-8) 9273 6400 Fax: (61-8) 9273 6466

FAS JOB # 1455

CONTENTS

1. SURVEY OPERATIONS AND LOGISTICS.....	5
1.1 INTRODUCTION.....	5
1.2 SURVEY BASE.....	5
1.3 FLYING SUMMARY	5
1.4 SURVEY PERSONNEL	5
1.5 AREA MAPS	5
1.6 SURVEY EQUIPMENT	7
2. SURVEY SPECIFICATIONS AND PARAMETERS.....	7
2.1 AREA CO-ORDINATES.....	7
2.1.1 Liverpool Project Area	7
2.2 SURVEY AREA PARAMETERS	7
2.3 DATA SAMPLE INTERVALS.....	8
2.4 SURVEY TOLERANCES	8
3. SURVEY EQUIPMENT AND SPECIFICATIONS	8
3.1 AIRCRAFT	8
3.2 AIRCRAFT DATA ACQUISITION SYSTEM.....	8
3.2.1 PDAS1000 Data Acquisition System.....	9
3.2.2 Processing Boards.....	9
3.2.3 PDAS1000A Power Console.....	9
3.3 NAVIGATION SYSTEM	9
3.3.1 PNAV2100 Navigation System.....	9
3.3.2 Aircraft GPS Receiver.....	10
3.3.3 Differential GPS Demodulator.....	10
3.3.4 Data Checking.....	10
3.3.5 Data Displayed and Recorded.....	11
3.4 AIRCRAFT MAGNETOMETERS AND CURRENT SENSORS	11
3.4.1 Caesium Vapour Magnetometer Sensor	11
3.4.2 Power circuit.....	11
3.4.3 Transputer Magnetometer Processor Board.....	11
3.4.4 Fluxgate Magnetometer.....	12
3.4.5 Current Sensors.....	12
3.4.6 Data Checking.....	12
3.4.7 Data Displayed and Recorded.....	12
3.5 GAMMA RAY SPECTROMETER SYSTEM.....	12
3.5.1 Data Checking.....	13
3.5.2 Data Displayed and Recorded.....	13
3.6 ARGUS - OARS (OPERATIONAL AIRBORNE REMOTE SPECTROMETER) SYSTEM	13
3.6.1 Data Checking.....	14
3.7 RADAR ALTIMETER	14
3.7.1 Data Checking.....	14
3.7.2 Data Displayed and Recorded.....	14
3.8 BAROMETRIC ALTIMETER	15
3.8.1 Data Checking.....	15
3.8.2 Data Displayed and Recorded.....	15
3.9 TEMPERATURE AND RELATIVE HUMIDITY SYSTEM.....	15
3.9.1 Data Checking.....	16
3.9.2 Data Displayed and Recorded.....	16
3.10 VIDEO TRACKING SYSTEM	16
3.11 FLIGHT DATA RECORDING	16
3.12 TIME BASE.....	17
3.13 FLIGHT FOLLOWING.....	17
4. GROUND DATA ACQUISITION EQUIPMENT AND SPECIFICATIONS	18

4.1	MAGNETIC BASE STATION	18
4.1.1	G-856	18
4.1.2	Magnetic Base Station Location	18
4.2	GPS BASE STATION SYSTEM	18
4.2.1	GPS Base Station Location	18
4.2.2	GPS Base Station Description	18
5.	EQUIPMENT CALIBRATIONS AND DATA ACQUISITION CHECKS	18
5.1	SURVEY CALIBRATIONS	18
5.1.1	Dynamic Magnetometer Compensation	19
5.1.2	Parallax	19
5.1.3	Radar Altimeter Calibration Line	20
5.1.4	Background and Cosmic Calibration Stacks	20
5.1.5	Height Attenuation Calibrations	20
5.1.6	Daily Calibrations	20
6.	SURVEY LINE NUMBERING SYSTEM	22
6.1	SURVEY LINE NUMBERING	22
6.1.1	Digital data	22
6.1.2	Flight logs	22
6.2	CALIBRATION LINE NUMBERING	23
6.2.1	Digital data	23
6.2.2	Flight logs	23
7.	DATA VERIFICATION AND FIELD PROCESSING	24
7.1	FIELD PROCESSING EQUIPMENT	24
7.2	MAGNETIC DIURNAL DATA	24
7.3	ALTIMETER DATA	24
7.3.1	Radar Altimeter Data	24
7.3.2	GPS Height Data	24
7.3.3	Barometric Altimeter Data	24
7.3.4	Topographical Data	24
7.3.5	Gridding and Inspection	24
7.4	FLIGHT PATH DATA	25
7.5	MAGNETIC DATA	25
7.5.1	Diurnal Correction	25
7.5.2	Parallax Correction	25
7.5.3	Preliminary Gridding and Inspection	25
7.6	SPECTROMETER DATA	25
7.6.1	Preliminary Corrections	25
7.6.2	Parallax Correction	25
7.6.3	Preliminary Gridding and Inspection	25
7.7	OARS DATA	25
7.8	DIGITAL ARCHIVES	26
8.	FINAL DATA PROCESSING	27
8.1	RAW DATA COLLECTION	27
8.1.1	Aircraft Data	27
8.1.2	Magnetic Base Station Data	27
8.1.3	Global Positioning System Base Station Data	27
8.2	AIRCRAFT LOCATION	27
8.3	MAGNETIC DATA PROCESSING	27
8.4	RADIOMETRIC DATA PROCESSING	28
8.4.1	Dead-Time Correction	28
8.4.2	Energy Calibration	28
8.4.3	Window Definitions	29

8.4.4	Cosmic Aircraft Background Removal	29
8.4.5	Atmospheric Radon	29
8.4.6	STP Altitude	29
8.4.7	Spectral Stripping	30
8.4.8	Height Correction	30
8.5	ARGUS DATA PROCESSING	30
8.6	DIGITAL ELEVATION MODEL	31
8.7	GRIDDING	31
APPENDIX I - FLIGHT PLAN		32
APPENDIX II – DAILY PRODUCTION REPORTS		33
APPENDIX III – FLIGHT SUMMARY		34
APPENDIX IV – LIST OF ALL SUPPLIED DATA		36

1. SURVEY OPERATIONS AND LOGISTICS

1.1 Introduction

Between October 2000 and January 2001 Fugro Airborne Surveys Pty. Ltd. undertook an airborne hyperspectral, magnetic and radiometric survey. The survey was part of a jointly funded exploration and research project between Cameco Australia Pty. Ltd., the Department of Mines and Energy Northern Territory (NT DoME) and Fugro Airborne Surveys Pty Ltd, over the Liverpool Project Area in the north west of Arnhem Land, approximately 45 km east of Jabiru. The survey area can be located on the SW corner of the 1:250,000 Milngimbi Australian Map Sheet (SD53-2), and the NW corner of 1:250,000 Mount Marumba Australian Map Sheet (SD53-6). The survey was flown using a Cessna 404 Titan / Courier owned and operated by Fugro. This report summarises the procedures, details and equipment used by Fugro in the acquisition, verification and processing of the airborne geophysical data.

1.2 Survey Base

The survey was based out of the township of Jabiru. The survey aircraft was operated from the Jabiru airport with the aircraft fuel available on site. A temporary office was set up in a room in the local hotel where all survey operations were run from and the post-flight data verification and processing was performed.

1.3 Flying Summary

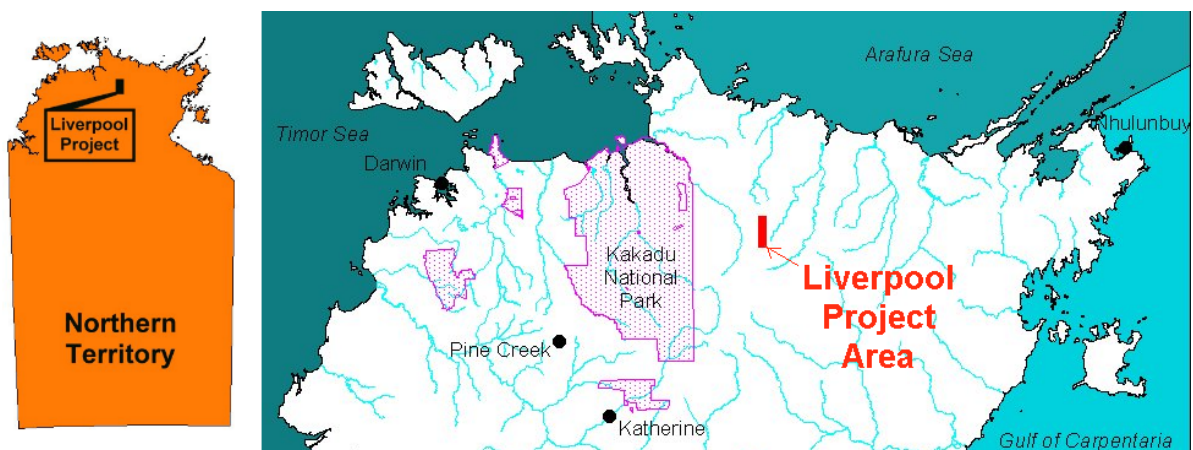
The terrain over most of the area was very flat, parts of the Liverpool area were somewhat hilly, with very little relief and sparse vegetation. The weather was generally hot and turbulent with temperatures in the high 30's and afternoon thunderstorms. It was cloudy at times but visibility for survey was generally very good.

1.4 Survey Personnel

The following personnel were involved on this project:

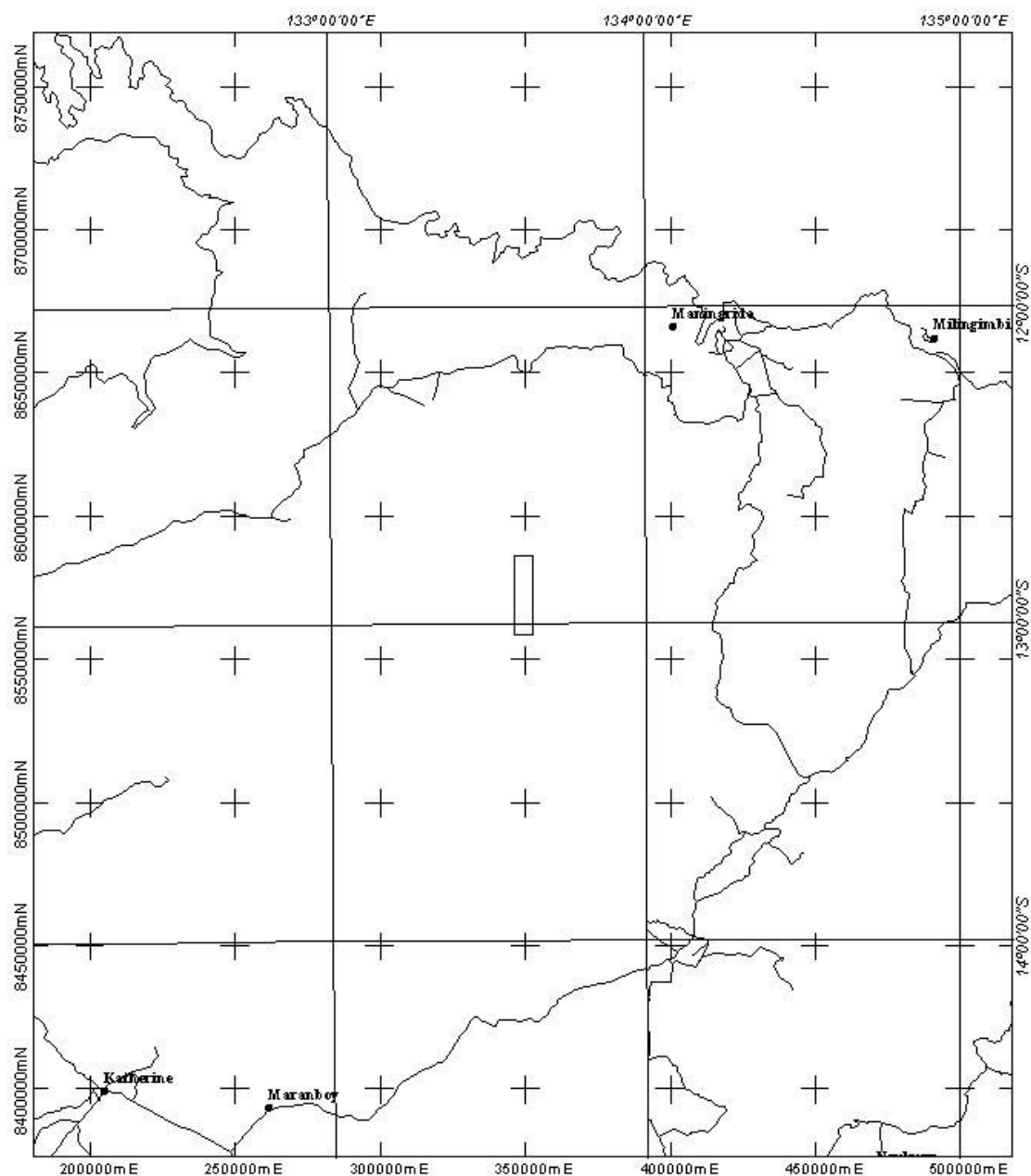
Project Manager/s (Perth)	Davin Allen
On-site Crew Leader/s	Matt Trevenen
Pilots	Peter Hall
System Operators	John Stewart
On-site Data Processing	Matt Trevenen
Data Processing (Perth)	Peter Chambers, Stuart Baron-Hay, Pavel Jurza

1.5 Area Maps



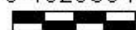
Location of the Liverpool Project within the Northern Territory

Location and flight planning information for the Liverpool Project



Location Plan for Cameco
Liverpool Project
Job 1455

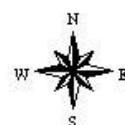
0 10203040 Kilometers



1:2000000

Projection : Transverse Mercator
Spheroid : WGS 84
FalseEasting : 500000
FalseNorthing : 10000000
CentralMeridian : 135

Flight Line Heading : 0
Flight Line Spacing : 100
Cross Line Heading : 90
Cross Line Spacing : 1000
Total Line Km : 2059



1.6 Survey Equipment

Survey Platform	-	Cessna 404 Titan / Courier
Data Acquisition System	-	Picodas Inc.PDAS-1000
Acquisition Software	-	Picodas / Fugro (in-house)
Magnetometer	-	Scintrex CS-2 Caesium vapour magnetometer
Fluxgate Magnetometer	-	Bartington model Mag-3 tri-axial fluxgate magnetometer
Spectrometer	-	Picodas PGAM 1000
Aircraft System GPS	-	Novatel GPS card
Aircraft Navigation System	-	Picodas PNAV
Real-time DGPS Receiver	-	Fugro Omnistar
Radar Altimeter/s	-	Collins ALT-50
Visual Tracking Camera	-	Panasonic WV-CD22
Visual Tracking Recorder	-	Panasonic AG-1070dc
Magnetic Base Stations	-	Primary: Geometrics G-856 Proton Magnetometer
	-	Backup: Geometrics G-856 Proton Magnetometer
Base GPS	-	Ashtech
Base Logging Computer	-	IBM Compatible Pentium Notebook
Processing Computer	-	HP Pentium Notebook / IBM compatible Pentium PC
Processing Software	-	Fugro (in house) & Geosoft Oasis Montaj

Hyperspectral Survey Equipment:-

Operational Airborne Research Spectrometers (OARS) - upward looking sensor with diffuser
- downward looking sensor

Prototype Thermal Infrared Profiling Spectrometer (TIPS)

Additional Picodas PDAS 1000 acquisition system to record OARS data

2. SURVEY SPECIFICATIONS AND PARAMETERS

2.1 Area Co-ordinates

The survey area was located within Australian Map Grid zone 53.
(Note - Co-ordinates in Australian Geodetic Datum Australia 1984)

2.1.1 Liverpool Project Area

Boundary 1	346227	8586281	-12.784399	+133.583320
Boundary 2	352546	8586281	-12.784705	+133.641524
Boundary 3	352546	8558759	-13.033509	+133.640180
Boundary 4	346227	8558759	-13.033197	+133.581918

2.2 Survey Area Parameters

Job Number	1455
Survey Company	Fugro Airborne Surveys Pty Ltd
Date Flown	October 2000
Client	Cameco Australia Pty Ltd
Area Name	Liverpool Project Area
Line kilometres	2000 kilometres
Traverse Line Spacing	100 metres
Tie Line Spacing	1000 metres
Traverse Line Direction	000 – 180 degrees
Tie Line Direction	090 – 270 degrees
Terrain Clearance	80 metres

2.3 Data Sample Intervals

Average data sample intervals.

Magnetometer	-	7.7 m (@10 Hz)
Radar altimeter	-	7.7 m (@10 Hz)
Temperature	-	7.7 m (@10 Hz)
Pressure	-	7.7 m (@10 Hz)
GPS	-	77 m (@1 Hz)
Spectrometer	-	77 m (@1 Hz)
OARS and TIPS data	-	77 m (@1 Hz)
Magnetic base station(G-856)	-	5 s

2.4 Survey Tolerances

As specified in the contract the following tolerances were used:

Traverse line separation	-	150 % of nominated line spacing over 5 km or more
Tie line separation	-	150 % of nominated tie line spacing over 5 km or more
Terrain clearance deviation	-	+/-20 m of nominal terrain clearance over 5 km or more
Total magnetometer system noise	-	More than 0.1 nT continuously over 1 km or more
Traverse line diurnal variation	-	More than 5 nT in 5 minutes in a non-linear fashion.
Tie line diurnal variation	-	More than 5 nT in 5 minutes in a non-linear fashion
Diurnal noise	-	More than 0.5 nT for 5 minutes or more

3. SURVEY EQUIPMENT AND SPECIFICATIONS

3.1 Aircraft

Specifications

Manufacturer	-	Cessna
Model	-	404 Titan / Courier
Registration	-	VH-WGB (Australia)
Ownership	-	Fugro Airborne Surveys Pty Ltd
Serial No.	-	404-0435
Year of Manufacture	-	1979
Engine/s	-	Twin, GTSIO-520m continental piston type
Propellers	-	Twin, 3 blade variable pitch McCauley 3FF 32C501
Dimensions	-	Wingspan 14.12 m
	-	Length 12.05 m
	-	Height 4.04 m
Fuel	-	Type - Avgas 100
	-	Capacity - Main tanks 346 US gallons (1317 litres)
	-	Endurance - @ 35 US gallons/hr = 10 hrs (with aux. fuel)
Seating	-	Survey configuration - 4 seats.
Flight Instruments	-	Cessna 400 series auto pilot
	-	Bendix / King KY196ATSO Com VHF radios x 2
	-	Bendix / King KYKY53TSO Nav VHF radios x 2
	-	Bendix / King KR87TSO ADF VHF radios x 2
	-	Bendix / King multi-channel HF radio
	-	Bendix / King KT-71 transponder
	-	Bendix / King RPR2000 colour weather radar
	-	Bendix / King DME
	-	Collins Alt 50 radar altimeter
	-	TRT radar altimeter
	-	Garmen GPS 100
	-	1 x Thrane Inmarsat-C unit
	-	Sigtronics intercom
	-	Slaving compass coupled to autopilot

3.2 Aircraft Data Acquisition System

The main body of this system is the PICODAS (PDAS) computer which is coupled to a GPS receiver for timing. The GPS receiver is connected to a PICODAS navigation console (PNAV) which displays to the pilot a graphical representation of the line being flown. The PNAV has a flight plan with area boundaries including the start and end of the line co-ordinates loaded into memory via a pre recorded flight plan. The PNAV outputs to the acquisition computer the position co-ordinates and other relevant GPS information. A PICODAS 1000A-interface console powers the magnetometer, spectrometers, fluxgate magnetometer, barometric altimeter and other analogue channels. The acquisition computer also outputs line number, direction, current position and fiducial to a VHS video recorder which records the ground track of each line.

3.2.1 PDAS1000 Data Acquisition System

The Picodas PDAS1000 data acquisition system is the central airborne data logging system. The PDAS computer executes a proprietary survey program for data acquisition and recording, and it executes required calibration procedures on all acquisition equipment. The data is presented both graphically and numerically in real time on a LCD display for both verification and quality control. The windows contain information for the operator to ensure the airborne systems are calibrated and functioning correctly.

All data is stored to a hard disk drive on the PDAS1000 with the main data being in binary file format. Additional information is stored in log files, text files, raw GPS files and spectrometer files. Data is removed from the aircraft system via magneto-optical disk which enables the data to be transferred to a field processing computer.

Specifications

Model	-	Picodas PDAS1000
Motherboard	-	Teknor Viper 807
Processor	-	Intel i486DX100
Operating System	-	MS-DOS 6.22
Storage	-	Hard disk - 1.2 GB (min)
Floppy disk	-	1.44 MB
Backup disk	-	640 MB Magneto-optical disk

3.2.2 Processing Boards

Three input transputer magnetometer processor board
 12 channel, 16-bit differential input, analogue processor board
 Three input PGAM spectrometer master transputer board
 12 channel Novatel GPS card
 Video overlay card
 Teknor VIPer807 i486DX100 motherboard
 Picodas display interface board

3.2.3 PDAS1000A Power Console

A PDAS1000A power console is used in conjunction with the PDAS1000. This console contains the auxiliary power supplies to provide regulated power to the acquisition sensor instruments. This unit contains backup power supplies for the Caesium magnetometer. This unit interfaces all the analogue signals to the PDAS1000 analogue board.

3.3 Navigation System

3.3.1 PNAV2100 Navigation System

The Picodas PNAV2100 Navigation computer is used for real time navigation with RTDGPS corrected position data received from the GPS card. The PNAV computer loads a pre-programmed flight plan from a disk which contains boundary co-ordinates, line start and end co-ordinates and line spacing and cross track display scales. The client information, spheroid, boundary information, master point and line spacing are stored in a configuration file. This information is transformed to the local co-ordinate system for calculation of cross track, distance to go and in/out of area information. This information, along with ground heading and ground speed is displayed to the pilot numerically and graphically on a pilots crosstrack display.

Differential update status is displayed to allow the pilot to assess the validity of the correction. In fixed wing aircraft the crosstrack information is also displayed on the aircraft horizontal situation indicator (HIS).

Information is also presented on an LCD display which gives a pictorial representation of the survey area, survey lines, and ongoing flight path.

The PDAS1000 and PNAV2100 are interlocked to enable autoselection and verification of the line to be flown.

Specifications

Model	-	Picodas PNAV2100
Motherboard	-	Axiom
Processor	-	Intel i486DX100
Operating system	-	MS DOS 6.22
Displays	-	LCD backlit display
	-	2 line LCD backlit display
	-	Horizontal situation indicator

3.3.2 Aircraft GPS Receiver

The Novatel GPS Receiver is used for airborne positioning and navigation and survey system timing. The GPS receiver is contained in the PDAS1000 computer and provides positional and satellite range data via the computer bus for display, recording and positional data via a serial port to the PNAV2100 for navigation. The GPS card accepts RTCM104 differential corrections via a serial port for real time differential solutions. Satellite range data is recorded for generating post-processed differential solutions.

GPS information is displayed on the PDAS1000 in real time giving information on each satellite being tracked and all relevant receiver diagnostics. The PDAS1000 also shows the accuracy of the GPS position and the status of the differential update. The survey acquisition software will only record satellite data for fixes greater than 4 satellites

Specifications

Model	-	Novatel 3951R GPS Receiver
Channels	-	12
Position update rate	-	PDAS1000 @ 1 Hz
	-	PNAV2100 @ 1 Hz
Raw data update rate	-	1 Hz
Datum	-	User selectable
Time sync	-	1 PPS output
Position accuracy	-	50 cm (CEP)

3.3.3 Differential GPS Demodulator

The Omnistar differential GPS service is utilised for providing real-time differential corrections via the Optus satellite network. These corrections are received at the aircraft using a Omnistar 3000L demodulator and the data from the selected reference station is passed to the GPS card via a serial link. Status of the real-time DGPS link can be monitored on the receiver and on the PDAS1000 display.

Specifications

Model	-	Omnistar 3000L
Received update rate	-	1-5 sec
Data format	-	RTCM 104 Ver .2

3.3.4 Data Checking

Data checking in the system is carried out automatically by the survey software and by real time display. The acquisition system will not allow GPS data to be collected for fixes of less than 4 satellites. The acquisition system will also display in real time the PDOP, HDOP, VDOP, TDOP, satellite azimuth, elevation and range. The survey system will allow any satellites, which may cause a distortion in the position to be locked out (i.e. low elevation). The survey system will also

display the status of the differential update and the accuracy of the position fix in real time. The survey system will display to the operator any errors encountered in the navigation system.

3.3.5 Data Displayed and Recorded

Data Displayed	Unit	Label	Recorded
GPS week	-	WEEK	Y
GPS time	sec	TIME	Y
Latitude	deg	LAT	Y
Longitude	deg	LONG	Y
Altitude	m	H_MSL	Y
Latitude RMS position error	m	STDLAT	Y
Longitude RMS position error	m	STDLOX	Y
Height RMS position error	m	STDHT	Y
Horizontal RMS position error	m	HRMS	N
Vertical RMS position error	m	VRMS	N
Position dilution of precision	-	PDOP	Y
Horizontal dilution of precision	-	HDOP	N
Time Shift dilution of precision	-	TDOP	N
Vertical dilution of precision	-	VDOP	N
Horizontal speed	m/s	VDOP	Y
Vertical speed	m/s	VDOP	Y
Horizontal heading	deg	VDOP	Y
GPS satellites	-	GPSS	Y
GLONASS satellites	-	GLOS	N
Navigation X	m	NAVX	N
Navigation Y	m	NAVY	N
Navigation Z	m	NAVZ	N
Satellite azimuth	-	raw	Y
Satellite range	-	raw	Y
Satellite status	-	raw	Y
Satellite signal	-	raw	Y

3.4 Aircraft Magnetometers and Current Sensors

3.4.1 Caesium Vapour Magnetometer Sensor

The caesium vapour magnetometer sensor is fitted in a tail mounted, kevlar/carbon fibre constructed airborne stinger. The sensor head is fixed in a Fugro universal sensor mount that allows for optimum alignment in any magnetic field. The sensor electronics are mounted in the base end of the stinger.

3.4.2 Power circuit

The magnetometer is powered by a dedicated isolated power supply in the PDAS1000A power console. Power is connected to the magnetometer using low loss coaxial cable. The Lamor frequency output of the magnetometer is modulated onto this power cable for input to the transputer magnetometer processor board in the PDAS1000. Remote hemisphere switching can be controlled electronically via switching to the magnetometer sensor.

Specifications

Model	-	Scintrex CS-2
Operating voltage	-	30 V DC
Operating range	-	15,000 - 100,000 nT
Sensitivity	-	0.001 nT
Heading error	-	+/- 0.25 nT
Noise envelope	-	0.002 nT pk-pk
Gradient tolerance	-	40,000 nT/m

3.4.3 Transputer Magnetometer Processor Board

The transputer magnetometer processor board provides frequency conversion for up to three input signals. The TMAG uses advanced transputer technologies allowing multi-tasking, multi-

processing and floating-point calculations giving advanced resolutions. The TMAG board is timed with the GPS PPS signal to derive precise frequency counting on the three PLD counters. Onboard signal processing status is displayed by LED, whilst system diagnostics are displayed in the survey program. The TMAG processing board interfaces with the PDAS1000 computer and the survey program, which initiates data sampling and transfers. Data is collected at 10 Hz for real time acquisition and sub sample data can be collected at 1 kHz. Barometric pressure and temperature are processed on the second and third inputs.

Specifications

Model	-	Fugro TMAG
Input range	-	15,000 - 100,000 nT
Resolution	-	0.5 pT
Sample rate	-	10 Hz Real-time acquisition
	-	1 kHz Sub-sample data
Transputer speed	-	30 MHz

3.4.4 Fluxgate Magnetometer

A Bartington three axis fluxgate magnetometer is used to determine the aircraft attitude. Each channel is recorded by the data acquisition system and can be displayed on the PDAS1000. This data is used to calculate compensation coefficients to remove all permanent magnetisation and induced magnetisation due to aircraft manoeuvres.

Combined with a compensation file the PDAS1000 can display and record real time TMI compensation data.

Specifications

Model	-	Bartington MAG-03M
Scaling Value	-	100 uT
Measuring Range	-	+/- 100 uT
Sample Rate	-	10 Hz

3.4.5 Current Sensors

Current sensors are used in the acquisition system to monitor any changes to the aircraft electrical system. These sensors will pick up changes in current that can cause spikes and level shifts in the magnetic data and unwanted electrical noise from aircraft radio and navigation systems. Current sensors are placed on each aircraft engine alternator and on the survey equipment rack.

3.4.6 Data Checking

Data checking is carried out in the survey system by displaying all available magnetic traces in real-time on the PDAS1000 display. Any errors detected by the survey system will be displayed to the operator.

3.4.7 Data Displayed and Recorded

Data Displayed	Unit	Label	Recorded
Raw Uncompensated TMI data	nT	TMAG1	Y
Compensated TMI data	nT	TCMA1	Y
Fourth Digital Difference of TMI data	pT	TFDD1	N
First Vertical Derivative of TMI data	pT/m	1VD	N
First Digital Difference of TMI data	nT	1DD	N
Ratio of TMAG1 and Fluxgate	nT/mV	RATIO	N
X axis Fluxgate	mV	XDEV	Y
Y axis Fluxgate	mV	YDEV	Y
Z axis Fluxgate	mV	ZDEV	Y
TMI Fluxgate	mV	FGATE	N

3.5 Gamma Ray Spectrometer System

The Picodas Gamma Ray Spectrometer system is utilised for airborne radiometric data acquisition. The system consists of two shock mounted fibreglass/Perspex casings, each containing four NaI (TI)

Crystals, giving a system volume of 33.56 litres. Each individual crystal has its own signal processing circuitry consisting of high and low voltage power supplies, analogue to digital conversion unit, EEPROM for storage of calibration coefficients and supporting circuitry for peak detection including adjustable threshold and coincidental peak recognition.

Each crystal pack has a slave transputer processing circuit for event processing and transferring each individual crystal spectra to the master transputer contained in the PDAS1000. The master transputer performs real time gain corrections on the individual spectra based on the tracking of the TI-208 (Th), K-40 or U photo peaks. Real time non-linearity corrections are applied according to individual coefficients determined during calibration under controlled conditions. For normal survey operation the summed 256-channel spectrum is transferred to the PDAS1000 for display and recording. Data can be displayed in real time showing individual crystal tracking statistics and crystal energy spectrums.

For pre and post-flight calibrations, the 256-channel spectrum for individual crystals are transferred for resolution determination and verification. In addition to the 256 channel summed spectra, individual energy windows may be defined for display and recording to the PDAS1000. These windows can be any of the IAEA defined energy windows or user selectable windows.

Raw 1024 channel individual crystal data is stored by the survey program as compressed spectra files. These files contain all the raw tracking information from each crystal. This data is used to post-energy calibrate any crystal peaks to obtain optimum performance.

All data recorded in the spectrometer system is dead time corrected and normalised to one second.

Specifications

Model	-	Picodas PGAM1000
Detector Volume	-	33.56 litres
Energy Channels Processed	-	1024
Energy Channels Recorded	-	256 summed data
	-	1024 compressed individual crystal data
Lower Energy Threshold	-	50 keV
Upper Energy Threshold	-	3000 keV
Cycle Rate	-	1 Hz

3.5.1 Data Checking

Data checking in the survey system is carried out by the use of resolution procedures using known radiometric sources to verify system, real time display of individual crystal resolutions and system resolutions whilst surveying, real time display of raw and corrected peak channel tracking information, real time display of the energy spectrum showing counts, cosmic level and coincident pulse counts. The survey system will display to the operator any errors encountered in the spectrometer system

3.5.2 Data Displayed and Recorded

Data Displayed	Unit	Label	Recorded
Spectrometer Statistics	-	SpStat	Y
Acquisition Time	ms	AcTime	Y
Total Counts	cps	TC	Y
Potassium Counts	cps	K	Y
Uranium Counts	cps	U	Y
Thorium Counts	cps	Th	Y
Cosmic Counts	cps	C	Y
256 Channel Data	cps	TC	Y
Raw Peak Channels	-	XtalSt	Y
Corrected Peak Channels	-	XtalSt	Y
Individual Crystal Statistics	-	XtalSt	Y

3.6 ARGUS - OARS (Operational Airborne Remote Spectrometer) System

OARS is comprised of two highly sensitive optical spectrometers viewing upwards and downwards and operating in line-scan (or profiling) mode, as well as a CCD push-broom imager to acquire ground-truth information. The two profiling sensors have identical spectral and radiometric specifications, each being a triple grating spectrometer. OARS acquires spectral reflectance data from 100 rectangular sub-pixels per second. Although the field of view of these sub-pixels on the ground (at 100m altitude) is 0.4m in the direction of flight x 10m across-track, the forward motion of the aircraft during their 10ms acquisition time

increases their size to approximately 1m. When these are added in groups of ten, the effective size of the ground pixel in the direction of flight is 10m. The 4-bit gain range of the CCD is also logged, yielding an effective dynamic range of 16 bits. This is sufficient to encompass the full range of solar irradiances and target albedos normally encountered, with usable signal to noise ratio. Both profiling sensors and the CCD imager are synchronised to the GPS second. There are always exactly 10 OARS integrated pixels and 80 CCD pixels per second. So there are exactly 8CCD pixels per OARS pixel.

Specifications

Model	- FUGROAR WGC100
Spectral Range	- 400 nm – 2500 nm
Spectrometer Type	- 3 grating spectrometers in each sensor
Downward sensor measurement	- ground target radiance (direct view through Herasil quartz window – uncoated)
Upward sensor measurement	- solar irradiance at aircraft (via diffuser cosine receptor and Herasil quartz window)
Wavelength Ranges and Detector Types	- VIS: Silicon 400 – 960 nm SWIR1: PbS 940 – 1760 nm SWIR2: PbS 1740 – 2500 nm
Number of CCD elements	- 256
Field of view at 100m altitude	- 88 degrees or 190 m across-track
Line scan rate	- 80 Hz

3.6.1 Data Checking

Data checking in the survey system is mostly operator free, however, if required the operator can interrupt or modify the data acquisition sequence. A good baseline is acquired by measuring a dark current block. The data acquired is interrupted by regular DC 'chops' to keep track of a varying baseline. When the end of the survey line is reached a 'bright' calibration is done, looking at an internal calibration light source, brought into the field of view by flip mirrors. The technique of having these long and short calibration cycles proves to be an effective way of keeping instrument performance up to laboratory standards.

3.7 Radar Altimeter

To maintain accurate minimum survey height clearance a COLLINS ALT-50 system is used. Data from this unit is recorded and displayed on the PDAS1000 for accurate terrain clearance. This information is displayed on a pilot instrumentation with low altitude warning annunciators set from a dialled up height. The height voltage is also displayed and recorded on the PDAS1000 in the form of raw mV height and a calculated altitude in either feet or meters. This height is calculated with a calibration procedure that accurately converts the voltage to an equivalent height.

Specifications – Collins Alt 50

Model	- Collins ALT50
Range	- 0-2000 ft
Accuracy	- 0 - 200' +/- 6' - 200-500' +/- 2 % - 500 - 2000' +/- 3.5 %
Sample Rate	- 10 Hz

3.7.1 Data Checking

Data checking is carried out in the survey system by displaying the radar altimeter information in real-time on the PDAS1000 display. Any errors detected by the survey system will be displayed to the operator.

3.7.2 Data Displayed and Recorded

Data Displayed	Unit	Label	Recorded
Raw input voltage Rad 1	mV	RRAD	Y
Radar height Rad 1	ft	RAD	Y

3.8 Barometric Altimeter

The output of the Digiquartz pressure transducer is used for calculating the barometric altitude of the aircraft. The atmospheric pressure is taken from a gimbal-mounted probe and fed to the transducer. The transducer uses a precise Quartz crystal resonator whose frequency of oscillation varies with pressure induced stress. The frequency is processed on the second channel of the transputer magnetometer board. The temperature of the pressure sensor is also recorded. In conjunction with the area QNH pressure and ambient temperature, the barometric altitude is calculated. This calculated altitude and the raw frequency are recorded and displayed on the PDAS1000.

Specifications

Model	-	Digiquartz 215A-101
Range	-	0 – 0.1 MPa
Accuracy	-	0.01 %
Resolution	-	1×10^{-8} Pa
Sample Rate	-	10 Hz

3.8.1 Data Checking

Data checking is carried out in the survey system by displaying the Digiquartz information in real-time on the PDAS1000 display. Any errors detected by the survey system will be displayed to the operator.

3.8.2 Data Displayed and Recorded

Data Displayed	Unit	Label	Recorded
Pressure frequency	Hz	PFREQ	Y
Temperature frequency	Hz	TFREQ	Y
Converted height	ft	HEIGHT	Y
Converted temperature	deg	DTEMP	Y

3.9 Temperature and Relative Humidity System

A Vaisala humidity/temperature sensor is utilised for measuring the relative humidity and temperature of the atmosphere external to the aircraft. The sensor produces a linear voltage that is measured by the analogue processor board in the PDAS1000

Specifications

Model	-	Vaisala HMP133Y
Sample rate	-	10 Hz
Relative Humidity	-	Measuring range - 0-100 % RH
Accuracy	-	+/- 1 %RH (0..90 %RH)
Sensor	-	HUMICAP H-Sensor
Temperature	-	Measuring range - -20 to +60 °C
Accuracy	-	+/- 0.2 °C
Sensor	-	Pt 100 RTD

3.9.1 Data Checking

Data checking is carried out by displaying the atmospheric information in real time on the PDAS1000 displays. Errors in the system will be displayed to the operator.

3.9.2 Data Displayed and Recorded

Data Displayed	Unit	Label	Recorded
Relative Humidity	RH	HUMID	Y
Temperature 2	deg C	TEMP2	Y

3.10 Video Tracking System

Fugro uses a colour video tracking system to allow recording of the flight path on a VHS-PAL videotape. The image data is recorded by a Colour CCD camera with an auto iris lens that is focused for optimum image. The video tape is synchronised with the recorded geophysical data by means of a video overlay card. The tape is overlaid with the PPS synchronised fiducial count, GPS position and line number. A video monitor is fitted onboard to allow the video data and timing information to be displayed. Time is displayed as a fiducial count that is synchronised with the GPS clock and time stamped on the data.

Specifications

Camera	Model	-	Panasonic WV-CL352
	Lens	-	HG4514FCS
	Footprint	-	60 m x 48 m
VCR	Model	-	Panasonic
	Format	-	VHS-PAL
Monitor	Model	-	Panasonic WV-5200

3.11 Flight Data Recording

All data recorded in the data acquisition system is stored in a digital format on the hard disk drive located in the PDAS1000. This data is then copied from the computer to a magneto-optical removable disk. The data is then transferred to the field processing computers for quality control examination.

Stored aircraft data consists of :

S.B files	-	Survey Binary files
S.T files	-	Survey Text files
R.R files	-	Raw Rover GPS files
P.C files	-	PGAM Compressed spectrometer files

Survey binary files contain:

Header	-	Line
	-	Flight
	-	Direction
	-	Date
ID group	-	Fiducial
	-	Time
AD group	-	Fluxgate data
	-	Raw radar altimeter data
	-	Ambient temperature data
	-	Relative humidity data
HT group	-	Converted barometric height
	-	Converted radar altimeter height
TM group	-	Raw TMI data
	-	Compensated TMI data
NO group	-	GPS time
	-	GPS week
	-	GPS real-time position
	-	GPS speed and direction
NS group	-	GPS position statistics
	-	GPS status
	-	Satellite channels
	-	Datum data

DP group	-	Barometric pressure frequency data
	-	Sensor temperature frequency data
	-	Converted height data
	-	Converted temperature data
SP group	-	Spectrometer statistics
	-	Total count window data
	-	Potassium window data
	-	Uranium window data
	-	Thorium window data
CH group	-	Cosmic window data
XS group	-	256 channel data
	-	Crystal statistics

Survey text files contain:

Survey and flight information in ASCII format

Rover GPS files contain:

Raw GPS data for post-flight processing

PGAM compressed spectrometer files contain:

Raw individual crystal data stored in 1024 channels per crystal

3.12 Time Base

The time base for this survey was based on the atomic clock output of the GPS satellites in all aspects of data acquisition. The aircraft acquisition system software is set to GPS time then adjusted to the local area time, in this case Australian Central Standard Time, whenever the system is initialised. The entire acquisition process is continuously locked to the "PULSE PER SECOND" hardware signal from the Novatel GPS card receiver(s), which itself is intrinsically slaved to GPS satellite time.

3.13 Flight Following

During the course of the survey the aircraft's position in real time was monitored using a Thrane & Thrane "CAPSAT" model INMARSAT-C/LM beacon installed on the survey aircraft. This equipment, with its independent GPS receiver, transmitted the position of the aircraft to a satellite over the Indian Ocean. This position was then relayed to Telstra via a ground station in The Netherlands. The aircraft's position is then logged on a computer at the Fugro office in Perth, which is connected permanently to a Telstra line.

The antenna for this equipment was located on top of the aircraft fuselage so as to achieve the best-unobstructed view of the satellite as possible. This equipment emits a high power (approx. 80W), near microwave, omni-directional signal and consequently draws high current from the aircraft electrical bus for a short period of time (3-4 ms). This current spike is detected as a spike in the aircraft's magnetic field by the magnetometer system and therefore is recorded in the magnetic data logged to disk. This interference is readily detectable in the 4th difference trace and occurs as a single pulse or as a 2 or 3 pulse burst about every 5-10 minutes or so.

4. GROUND DATA ACQUISITION EQUIPMENT AND SPECIFICATIONS

4.1 Magnetic Base Station

Geometrics G-856 proton base station magnetometers were used to monitor the magnetic diurnal variation. All magnetometers were synchronised to the local time base of the aircraft survey system GPS prior to surveying each day. Two G-856 magnetic base stations were set-up at Jabiru airport. Prior to positioning the base stations a mini-survey was conducted to establish a magnetically low gradient area. A base value for the primary base station was calculated and used in the diurnal correction of the magnetic data.

4.1.1 G-856

Model	- Geometrics G-856 proton memory magnetometer
Displays	- Six digit display of magnetic field to resolution of 0.1 nT or to nearest second. Additional three digit display of station, year and record number.
time	
day of	
Resolution	- Typically 0.1 nT in average conditions.
Absolute accuracy	- 1 nT, limited by remnant magnetism in sensor and crystal oscillator accuracy.
Clock	- Julian clock with stability of +/-2 seconds per day.
Memory	- Approximately 12,500 readings.
Output	- RS-232 output data in standard format.
Sample rate	- Internal logging at 5sec (0.2 Hz) rate.

4.1.2 Magnetic Base Station Location

The base station location is given in the WGS84 datum.

Base	Longitude	Latitude	Base value
Jabiru	132° 50' 10"	-12° 39' 52"	46470 nT

4.2 GPS Base Station System

4.2.1 GPS Base Station Location

A GPS base logging station was set up at the survey base office in Jabiru with the GPS antenna set in the following position:

(Note - co-ordinates are in the WGS84 datum):

Base	Longitude	Latitude	Height
Jabiru local hotel	132° 50' 10.25"	-12° 39' 51.96"	109.88 m

4.2.2 GPS Base Station Description

The GPS base system comprises a GPS receiver, a logging computer, an antenna and a UPS system to avoid down time if power fails or fluctuates. The GPS receiver is connected to the PC via a serial COM connector. Data is logged using proprietary software and displayed in real time on the screen.

Logged base data is processed in conjunction with the airborne GPS data to calculate the post-processed differential position of the aircraft.

Proprietary software is used to display and calculate flight path of the aircraft and altitude clearance.

Specifications

Ashtech G12 Receiver

Model	- Ashtech G12 Receiver
Receiver	- 12 Channel GPS code and carrier
Position Accuracy	- Differential mode <40 cm

5. EQUIPMENT CALIBRATIONS AND DATA ACQUISITION CHECKS

5.1 Survey Calibrations

A series of calibrations were performed as follows:

5.1.1 Dynamic Magnetometer Compensation

Carrying a magnetometer through a varying field in a non-uniform orientation produces manoeuvre noise. To compensate for this manoeuvre noise a standard compensation test flight called a “comp box” is flown. The compensation file produced also removes the majority of the heading error. Aircraft compensation tests were flown on the 4 survey line headings and also at $\pm 7\frac{1}{2}$ and 15° to the line headings (to accommodate for cross wind flying conditions). The data for each heading consists of a series of aircraft manoeuvres with large angular excursions: specifically pitches, rolls and yaws. This is done to artificially create the worst possible attitudes and rates of attitudinal change likely to be encountered while on line and compensate for any magnetic noise created by the aircraft’s motion within the earth’s magnetic field. This data is processed to obtain the real time compensation terms. These coefficients are applied in real-time and later during post-processing. Note that this form of compensation will only remove those noise effects modelled in the manoeuvre test flight. Random motions of the stinger with respect to the aircraft airframe generally establish the noise floor for this type of installation. A single comp boxes was flown at the start of the survey and as no change was made to the magnetic signature of the aircraft, e.g. 100 hourly service, equipment change or repair, etc, no further comp boxes were required.

Date flown	Flights covered
4/10/00	4,6 & 8

5.1.2 Parallax

Parallax error is caused by the physical difference in distance between the various sensors, the electronic delay and software timing in the acquisition system. Hence all variables are subjected to a displacement from the GPS co-ordinates. If these variables are processed without a position offset a parallax error will occur. The most suitable way to treat this problem is to use the 1 second radiometric data as a base with a zero correction. This will prevent interpolation of important variables (a filtering process). The co-ordinates were moved by linear interpolation and other data variables were displaced onto the radiometric data, without change, in multiples of 0.1 seconds.

5.1.2.1 Spectrometer

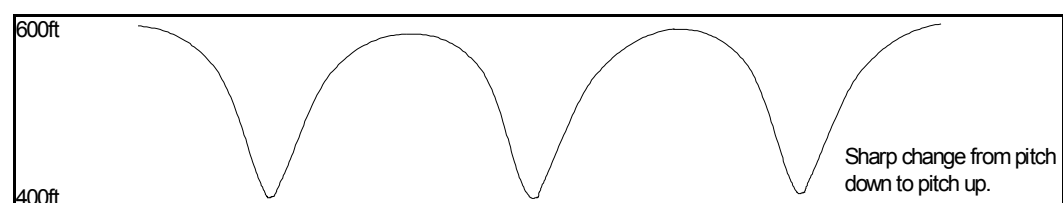
The spectrometer data were not parallaxed but a correction was made by applying a parallax to the co-ordinate data. This parallax was computed using a section of lines with a spacing of 100 metres and regridding the data until the appropriate amount of parallax was applied.

5.1.2.2 Magnetometer

The magnetometer parallax was computed using a section of lines with a spacing of 100 metres and regridding the data until the appropriate amount of parallax was applied.

5.1.2.3 Barometric and Radar Altimeter Parallax

In order for processing to accurately determine the parallax error associated with the barometric and radar altimeter data a parallax test line was flown. This line consisted of five sharp swoops between 600ft and 400ft. Starting at an altitude of 400ft the aircraft sharply descended to 400ft, then ascended upward to 600ft, levelling off for a few seconds before repeating this a further four times.



5.1.2.4 Data parallaxes

Data	Parallax
Radiometrics	0 seconds
GPS easting	-1.4 seconds
GPS northing	-1.4 seconds
GPS height	-1.4 seconds
Magnetics	-1.1 seconds
Radar altitude	-1.1 seconds
Pressure	-1.3 seconds
Temperature	0 seconds

5.1.3 Radar Altimeter Calibration Line

Height above the terrain is measured using a radar altimeter. The output voltage from the radar altimeter unit is recorded along with the survey data in the PDAS binary files. A look-up table is used to convert this output voltage into an altitude in metres. The lookup table is computed by recording the output voltage at various heights above the ground as indicated on the radar altimeter display.

5.1.4 Background and Cosmic Calibration Stacks

Radiometric data recorded by the PGAM 1000 is contaminated by various non-terrestrial sources. In order to provide an accurate representation of terrestrial (or natural) radiometric content these other sources must be identified and removed. This was done by flying a series of high level test lines over the ocean. Fixed barometric altitudes were flown for 5 minutes from 1000 ft above ground level (AGL) ascending at 2000 ft intervals up to and including 9000 ft A.G.L. then descending in the same manner.

5.1.5 Height Attenuation Calibrations

Gamma -rays are attenuated by air at approximately an exponential rate. It is therefore essential that corrections for aircraft altitude are incorporated into processing procedures. In order to correct for varying aircraft altitude and to accurately convert airborne counts into ground concentrations of potassium, uranium and thorium a series of height attenuation, or low level stacks, were flown. Over a calibration test line the stacks were flown starting at 150 ft and incrementing at 50 ft intervals to 450 ft, then 1000 ft, 1500 ft and 2000 ft with data recorded for 300 seconds at each level.

5.1.6 Daily Calibrations

A set of daily calibrations were performed each survey day as follows:

5.1.6.1 Magnetic Base Station Time Check

Prior to each days survey all magnetic base stations were time checked and synchronised with the time on the aircraft survey system GPS receiver. The temporal drift over a typical survey day of approximately 12 hours, was determined to be on the order of 1 second or less for all mag base stations.

5.1.6.2 Barometric Calibration

In order to correct the computed barometric height for pressure variations during the survey a correction is applied using a measured pressure at a known height. This pressure is known as QFE pressure and it was measured in the aircraft pre and post sortie at the airport. Barometric recorded for a period of 30 seconds.

5.1.6.3 Spectrometer Resolution Tests

Internal Quality Control of the Gamma-Ray Spectrometer (PGAM 1000) relies on continually monitoring the resolution and peak positions of individual crystals. Prior to and after each days survey a Thorium source was placed on the PGAM 1000 crystal pack in a designated location at least 50 cm from each detector pack with 120 seconds of resolution test data recorded.

5.1.6.4 Spectrometer Button Tests

Hand sample checks were performed on the spectrometer before and after each days survey acquisition. Each sample was placed in a predetermined location and data recorded for 60 sec. Relative count rates above background were within +/- 10% of the average sample checks for the duration of the survey.

5.1.6.5 Low Level Test line

To monitor the effects of soil moisture and radon and to verify the system was functioning correctly a low level test line was flown in a constant direction at survey altitude for 5 km prior to and after each days production. The collected data was checked by the operator to ensure the Total Count and Th. for the low level test line was within +/- 20% of the initial average.

6. SURVEY LINE NUMBERING SYSTEM

The following line numbering formula was employed for this survey, only the first 4 digits of the line number are shown:

Line No./Range	Type	Duration	Frequency	Comments
1503	Thorium source	180 seconds	Daily	A.M. spec. cals
1504	Background	180 seconds	Daily	A.M. spec. cals
1508	Low level test line	~5 km	Daily	A.M. spec. cals
1509	High level test line	300 seconds	Daily	A.M. spec. cals
1603	Thorium source	180 seconds	Daily	P.M. spec. cals
1604	Background	180 seconds	Daily	P.M. spec. cals
1608	Low level test line	~5 km	Daily	P.M. spec. cals
1609	High level test line	300 seconds	Daily	P.M. spec. cals
1511	Baro. altimeter	30 seconds	Pre sortie	1 st sortie
1611	Baro. altimeter	30 seconds	Post sortie	1 st sortie
1512	Baro. altimeter	30 seconds	Pre sortie	2 nd sortie
1612	Baro. altimeter	30 seconds	Post sortie	2 nd sortie
1811-1820	Comp box	~260 seconds	As required	
1831-1845	High level spec	300 seconds	Annually	Over water
1850-1865	Low level spec	5 km	Annually	Carnamah test range
1870-1874	Pad cals pack #1	300 seconds	Annually	Bg, K, U, Th
1875-1879	Pad cals pack #2	300 seconds	Annually	Bg, K, U, Th
4001-4065	Traverse line	As required		
4701-4728	Tie line	As required		

6.1 Survey line numbering

6.1.1 Digital data

All survey lines are stored as 5 digit integers in the digital data and take the form ANNNP where:

- A - Area number: for this survey either a 1, 2, 3 or 4.
- NNN - Line number: if the 1st digit is a 7 then the line is a tie line. e.g. **20140** is traverse line 14 from area 2, **17030** is tie line 3 from area 1.
- P - Attempt number: if a line is scrubbed and reflowed or flown in multiple parts the attempt number will be increment by 1. e.g. **20412** indicated the 3rd attempt for line 41 from area 2.

6.1.2 Flight logs

Survey lines written in the flight logs, and as displayed on video, are written in the form SANNN.PD where:

- S - Alphabetic descriptor: “ ” indicates a traverse line, “T” indicates a tie line, “S” indicates a scrubbed line.
- A - Area number
- NNN - Line number
- .
- P - Attempt number
- D - Direction: **N**orth, **S**outh, **E**ast or **W**est.

6.2 Calibration line numbering

6.2.1 Digital data

All calibration lines are stored as 8 digit integers in the digital data and take the form ANNNPFFF where:

- A - Area number: this is not important for a calibration line and is generally 1 for most calibration lines regardless of which block was being flown.
- NNN - Line number: as per the line number description table.
- P - Attempt number: unlike survey lines there are no part calibration lines
- FFF - Flight number: the flight number is appended to the line number as calibration lines are repeated during the survey.

6.2.2 Flight logs

Calibration lines written in the flight logs, and as displayed on video, are written in the form SANNN.PD where:

- S - Alphabetic descriptor: "C" indicates a calibration line, "S" indicates a scrubbed line.
- A - Area number
- NNN - Line number
- .
- P - Attempt number
- D - Direction: **N**orth, **S**outh, **E**ast or **W**est.

7. DATA VERIFICATION AND FIELD PROCESSING

All data verification and processing was conducted at the field office in Jabiru for the duration of the survey. At the conclusion of each days survey all magnetic, spectrometer, hyperspectral, altimeter, flight path and diurnal data was down-loaded onto the field office computer for preliminary verification.

7.1 Field Processing Equipment

IBM compatible Pentium computer with optical disk drive.
HP Pentium notebook.
Canon bubble jet printer.

7.2 Magnetic Diurnal Data

Diurnal data recorded every second from the primary base station was down-loaded from the magnetometer's base logging computer onto the field processing computer via a floppy disk. The data was then checked for spikes and erroneous readings. If invalid diurnal data occurred whilst survey data was being acquired the affected section was re-flown. The diurnal data was also checked to see that the change in diurnal readings during the course of the survey did not exceed the specified tolerances. When this occurred the affected part of the survey line was re-flown. The diurnal data was merged with the aircraft data and used in the verification of the magnetic data. Diurnal data recorded on the backup base station was also down-loaded onto the field processing computer directly via a dump cable.

7.3 Altimeter Data

Radar altimeter, barometric altimeter and GPS height data from the aircraft was transferred via magneto-optical disk onto the field processing computer.

7.3.1 Radar Altimeter Data

The radar altimeter is verified to check that a reasonably constant height above the terrain specified was flown, readings during the course of the survey did not exceed the specified tolerances and for equipment reliability. The radar altimeter data is used in the production of topographic maps.

7.3.2 GPS Height Data

The aircraft's height above mean sea level each second was determined by differentially post-processing the synchronised DGPS data from the aircraft and GPS base station. The GPS height of the aircraft is verified to check for data masking and for equipment reliability. The GPS height data is used in the production of topographical maps.

7.3.3 Barometric Altimeter Data

As a backup to the aircraft's GPS height barometric data was also recorded. The barometric height of the aircraft is verified to check for equipment reliability. The barometric data is also used in the processing of the spectrometer data.

7.3.4 Topographical Data

After verification parallax corrections were applied and the radar altimeter height was subtracted from the GPS height to give the elevation of the terrain above the GDA94 ellipsoid. It was not considered necessary to make any further corrections as this data is for verification purposes only.

7.3.5 Gridding and Inspection

The topographical data was gridded and grid image enhancements were computed and displayed on screen. These were inspected for inconsistencies and errors and appropriate corrections were made if required.

7.4 Flight Path Data

The flight path data from the aircraft and the GPS base station were transferred via magneto-optical disk onto the field-processing computer. The aircraft's precise location each second was determined by differentially post-processing the synchronised GPS data from the aircraft and GPS base station. The flight path was recovered and plotted daily to ensure it was within specification. Any data not within specification was re-flown. The flight path data was then merged with the rest of the aircraft and diurnal data. Both the aircraft and GPS base station recorded the data in the WGS 1984 datum.

7.5 Magnetic Data

The real-time compensated and uncompensated magnetic data from the aircraft recorded every 0.1 second were transferred via magneto-optical disk onto the field-processing computer. The raw, unedited magnetic data was checked to identify noise and spikes. Single reading spikes were manually edited and if the noise exceeded the specified tolerances the part of the line affected was re-flown. After the edited magnetic data was merged with the digital flight path the following sequence of processing operations were carried out to allow inspection and verification of the data:

7.5.1 Diurnal Correction

The synchronised digital diurnal data collected by the base station was first subtracted from the corresponding airborne magnetic readings to calculate a difference. The resultant difference was then subtracted from the base value to produce diurnally corrected magnetic data.

7.5.2 Parallax Correction

The diurnally corrected magnetic data was then corrected for system parallax using the calculated value.

7.5.3 Preliminary Gridding and Inspection

The magnetic data was gridded and grid image enhancements were computed and displayed on screen. These were inspected for inconsistencies and errors and appropriate corrections were made if required.

7.6 Spectrometer Data

Spectrometer data from the aircraft was transferred via magneto-optical disk onto the field-processing computer. The data is verified to check that readings during the course of the survey did not exceed the specified tolerances and for equipment reliability.

7.6.1 Preliminary Corrections

Standard radiometric data reduction corrections were then applied to the Total Count, Potassium, Uranium and Thorium window data.

7.6.2 Parallax Correction

The corrected window data were then corrected for system parallax using the calculated value.

7.6.3 Preliminary Gridding and Inspection

The spectrometer data was gridded and grid image enhancements were computed and displayed on screen. These were inspected for inconsistencies and errors and appropriate corrections were made if required.

7.7 OARS Data

OARS data from the aircraft was transferred via magneto-optical disk onto the field-processing computer. The data is verified to check that readings during the course of the survey did not exceed the specified tolerances and for equipment reliability.

7.8 Digital Archives

All raw aircraft data was backed up on magneto-optical disk at the end of each day's survey. Two copies of all verified and edited data were made onto magneto-optical disk also at the end of each day's survey. One copy was sent by courier to the Fugro office in Perth with the other copy remaining at the field processing office.

8. FINAL DATA PROCESSING

Three separate streams of raw data are collected by separate acquisition systems. All three sets of data are treated as discrete units and are post-processed accordingly before being merged.

8.1 Raw Data Collection

8.1.1 Aircraft Data

Data collected by the aircraft includes:

- TMI via the Caesium vapour magnetometer
- 1024 Channel spectrometer
- OARS (Operational Airborne Remote Sensing Spectrometer)
- 3 axis fluxgate magnetometer
- radar altimeter
- pressure
- temperature
- fiducial
- time
- GPS Positioning information (including time and satellite info.)

8.1.2 Magnetic Base Station Data

Whilst the aircraft was collecting data, magnetic diurnal data was collected at the aircraft base.

8.1.3 Global Positioning System Base Station Data

An Ashtech Ranger II 12 channel GPS receiver was used for the GPS base station at the crew headquarters. This instrument recorded variables such as location, time and satellite information to be used later for post-processing of the aircraft location.

8.2 Aircraft Location

The aircraft's location each second was determined by differentially post-processing the synchronised GPS data recorded on both the aircraft and GPS base station. Where small gaps occurred in the differential data, positions were calculated using the GPS velocity data. This data is recorded in the WGS84 datum. The WGS84 data was then transformed to the AGD84 datum using a seven parameter transformation. The transformation parameters used to transform from WGS84 to AGD84 were:

DX	DY	DZ	Xrot	Yrot	Zrot	Scale
116	50.47	-141.69	0.23	0.39	0.344	-0.0383E-6

Prior to being merged with the magnetic, radiometric, hyperspectral and topographic processing stream data, system parallax as calculated was applied.

8.3 Magnetic Data Processing

Data collected by each of the raw data sources is checked for spikes and noise by complex procedures. These procedures are summarised below:

- a) Apply any spike corrections (including Inmarsat transmissions) to the raw magnetic variables.
- b) Interpolate undefined magnetic values.
- c) Apply fluxgate corrections and compensate the data with post-processed compensation files.
- d) Filter diurnal values and subtract them from individual compensated magnetic readings. A diurnal base value was then added.
- e) Apply parallax correction.
- f) Co-ordinate the data with post-processed GPS data.
- g) Correct for regional effects of the earth's magnetic field by calculating the IGRF value at each fiducial using IGRF model 1995 and secular variation model. A base value was added back.

IGRF Model	Base Value
1995	46640 nT

- h) Using the tie lines (flown at 90 degrees to the traverse lines) a set of miss-tie values were determined. These miss-tie values reflected the differences in the magnetic value between the tie lines and the traverse lines over the same geographical point. Using a least squares fit algorithm, which also takes into account the statistical variation inherent in DGPS positioning, a series of corrections were applied to the traverse line data. These allowed the data to be levelled to the same base value.
- i) Following this, a Fugro proprietary micro-levelling process was applied in order to more subtly level the data. This process removes sub-gamma pulls evident only under image enhancement algorithms.

8.4 Radiometric Data Processing

The radiometric data was processed using the standard IAEA window processing technique as summarised below.

- a) The 1024 channel data is energy calibrated.
- b) Sum individual energy calibrated crystals to produce a total pack 256 channel spectrum.
- c) Window the 256 channel data using the IAEA standard energy windows.
- d) Co-ordinate the data with post-processed GPS data.
- e) Apply spike corrections to the radar altimeter, temperature and pressure values.
- f) Apply parallax corrections to altimeter, temperature and pressure data.
- g) Calculate the equivalent terrain clearance at STP (standard temperature and pressure).
- h) Remove aircraft background.
- i) Remove cosmic background.
- j) Remove radon background.
- k) Apply stripping ratios.
- l) Apply height corrections.

8.4.1 Dead-Time Correction

Gamma-ray spectrometers require a finite time to process each pulse from the detectors. While one pulse is being processed, any other pulse that arrives will be rejected. Consequently the 'live' time of a spectrometer is reduced by the time taken to process all pulses reaching the multi channel analyser. The Picodas PGAM 1000 system has analogue to digital converters associated with each detector, and as such, the total dead-time, even at ground level is extremely small, and as such was omitted.

8.4.2 Energy Calibration

The spectral drift was checked by monitoring the position of Potassium, Uranium and Thorium peaks on average spectra along flight lines. The peak positions were determined by removing the Compton continuum and applying a gradient search technique on the residual spectrum. The original 1024 channel data was mapped onto the corrected peak positions and a new 256 channel data set was generated by interpolation and summation.

To verify the calibration, spectra was checked by comparing the before and after energy calibration plots. Where any spectra showed errors in recalibration, or any other abnormalities, the lines were reflight.

8.4.3 Window Definitions

The 256 channel data were summed into the standard IAEA windows.

Window	Peak Energy (keV)	Energy Window (keV)		PGAM Channel Window	
Total Count	-	410	- 2810	34.9867	- 239.7867
Uranium Low	609	550	- 750	46.9333	- 58.0267
Potassium	1460	1370	- 1570	116.9067	- 133.9733
Uranium	1765	1660	- 1860	141.6533	- 158.7200
Thorium	2615	2410	- 2810	205.6533	- 239.7867
Cosmic	-	3000	- 6000	-	-

8.4.4 Cosmic Aircraft Background Removal

The cosmic and aircraft backgrounds for each channel are of the form:

$$N = a + b \cdot C$$

where

- N = combined cosmic & aircraft background in each spectral window
- a = aircraft background in the window
- C = cosmic channel count
- b = cosmic stripping factor

The aircraft background radiation was removed by subtracting the computed aircraft background from the Total Count, Potassium, Uranium and Thorium windows. The effect of cosmic radiation was removed from each window by multiplying the cosmic channel by the cosmic stripping factor for each window and subtracting the result from the window data.

Aircraft Background and Cosmic Stripping Ratio for VH-WGB

Window	Aircraft Background	Cosmic Stripping Ratio
Total Count	60.0	1.430
Potassium	8.4	0.079
Uranium	3.0	0.063
Thorium	1.5	0.070

8.4.5 Atmospheric Radon

The method of radon removal differs to that of Grasty and Minty (A Guide to the Technical Specifications for Airborne Gamma-Ray Surveys. Record 1995/60 p.34, Australian Geological Survey Organisation) and is proprietary but its effectiveness is evident in the quality of the final product.

8.4.6 STP Altitude

The radar altimeter data was converted to effective height at standard temperature and pressure using the expression:

$$STPAlt = RAlt * (P/103) * (273 / (T+273))$$

where:

- RAlt = the observed radar altitude in metres
- T = the measured air temperature in degrees C
- P = the barometric pressure in hectopascals

8.4.7 Spectral Stripping

Spectral stripping was applied to the Potassium, Uranium and Thorium windows. The stripping co-efficients were corrected for STP altitude.
Stripping Ratios for VH-WGB

Stripping	Value	STP adjustment (/m)
Alpha	0.2504	0.00049
Beta	0.3513	0.00065
Gamma	0.7394	0.00069
a	0.0391	0
b	0	0
g	0	0

8.4.8 Height Correction

The background corrected and stripped window data were then corrected for variations in the density altitude of the detector.

STP Altitude Coefficients for Aircraft VH-WGB

Window	Attenuation coefficient (m^{-1})
Total Count	-0.0067
Potassium	-0.0082
Uranium	-0.0084
Thorium	-0.0066

8.5 Argus Data Processing

The processing stream for Level 1 processing for ARGUSTM includes four steps and is applied to the full available spectral range of each instrument:

Step 1 - Collection and Organisation. Compile data from ALL of the acquisition systems into a single database.

Step 2 - Pre-processing Procedures. Correct data for instrument dependencies and produce output in recognisable physical units. This includes dark current subtraction, radiometric correction and reflectance processing. Reflectance processing includes application of atmospheric corrections (ATREM) for visible-near infrared and short wave infrared data; and calibrated radiance (using cold and warm black body calibration cycles) and apparent emissivity for thermal wavelength data.

Step 3 - Processing. This consists primarily of minimum noise fraction (MNF) and spectral unmixing techniques. In order to perform a reliable MNF transform, a subset of the data (using threshold values and other techniques) is chosen that excludes data with obvious non-mineral signatures (atmospheric artefacts, impact of clouds, humidity etc.).

Unmixing is a procedure that aims to reproduce spectral signatures which we can relate directly to minerals and vegetation, from MNF components. This step applies the N-dimensional visualiser (ENVI) to analyse the N-D scatter clouds. The results are edge-members or end-members that we identify by comparison with known mineral signatures from laboratory analysis (USGS spectral library).

Step 4 – Production. Data acquisition continues throughout the day under a range of conditions (clear blue sky to full cloud cover). Hence there is a wide range of changes in sun illumination, humidity, cloud cover etc. These changes produce offsets in data on a line by line basis that we currently remove by a de-corrugation/ micro levelling approach.

8.6 Digital Elevation Model

Data collected by each of the raw data sources is checked for spikes and then processed as follows:

- Apply any spike corrections to the raw radar altimeter data.
- Interpolate undefined values.
- Apply parallax correction.
- Co-ordinate the data with post-processed GPS data.
- Subtract the aircraft's height above ground from the aircraft's height above the WGS84 ellipsoid and correct for radar altimeter/GPS sensor separation.
- Convert to Australian Height Datum 1998 (AHD) by using the AUSLIG geoid model corrections for AHD 1998.
- Using the tie lines (flown at 90 degrees to the traverse lines) a set of miss-tie values were determined. These miss-tie values reflected the differences in the computed topographic height between the tie lines and the traverse lines over the same geographical point. Using a least squares fit algorithm, which also takes into account the statistical variation inherent in DGPS positioning, a series of corrections were applied to the traverse line data.

Following this, a Fugro proprietary micro-levelling process was applied in order to more subtly level the data.

8.7 Gridding

The final levelled magnetic, radiometric and elevation data were gridded using a cubic spline method. A grid cell size of 25 metres, ¼ line spacing, was used. Grids were made of Total Magnetic Intensity, Total Count, Potassium, Uranium, Thorium and Digital Elevation Model in ERMapper format.

APPENDIX I - Flight Plan

```

JOB Number      1455.4
CLIENT          CAMECO
AREA_NAME       Alligator River
PLANNED_BY      Matt Trevenen      05/10/2000 Boundary change lan
|
SPHEROID        3 AUSTRALIAN NAT. 6378160.0 298.25 0.9996
DELTAXYZ        116.00 50.47 -141.69 0.230 0.390 0.344 -0.0983E-6
HEMISPHERE      SOUTH
UTM_ORIGIN      53 135 135
BOUNDARY        1 346227 8586281 -12.784399 +133.583320 -124703.8 +1333460.0 12
BOUNDARY        2 352546 8586281 -12.784705 +133.641524 -124704.9 +1333829.5 12
BOUNDARY        3 352546 8558759 -13.033509 +133.640180 -130200.6 +1333824.6 12
BOUNDARY        4 346227 8558759 -13.033197 +133.581918 -130159.5 +1333454.9 12
SQUARE_KMS      173.912
|
NAVTYPE         NOVATEL
NAVMODE         U.T.M
PLAN_TYPE       Normal
LINE_TYPE       S.LINE X.LINE 0 0
HEADING         000 090
SPACING         100 1000 1000 1000
OVER_LINE       0 0
OVERFLY         500 500
MIN_LENGTH      5 5
FIRST_LINE      10 10
INCREMENT       10 10
X_TRACK         100 100
MASTER_PT       1 271000 8608600 -12.578077 +132.892205
MASTER_NEW      0 Not implemented.
KM_in_AREA      1789 177
KM+OVERFLY      1854 205

```


APPENDIX II – Daily Production Reports

JOB : 1455.4
 CLIENT : CAMECO
 AREA : Alligator River
 FLIGHT : 004
 JULIAN : 280
 DATE : 06/10/2000
 AIRCRAFT: VH-WGS

 ON LINE : 923.4 kms 3.149 Hrs
 SCRUB : 0.0 kms 0.000 Hrs
 OVERFLY : -67.7 kms
 PRODUCTION : 855.7 kms 3.149 Hrs
 TURN AROUND: 0.940 Hrs
 CALIBRATION: 0.000 Hrs
 FERRY : 0.911 Hrs

 TOTAL HOURS: 5.000 Hrs

 BACKED by Matt Trevenen on 10/10/2000

JOB : 1455.4
 CLIENT : CAMECO
 AREA : Alligator River
 FLIGHT : 006
 JULIAN : 283
 DATE : 0/2000
 AIRCRAFT: VH-WGS

 ON LINE : 1114.4 kms 3.804 Hrs
 SCRUB : 0.0 kms 0.000 Hrs
 OVERFLY : -87.6 kms
 PRODUCTION : 1026.8 kms 3.804 Hrs
 TURN AROUND: 1.068 Hrs
 CALIBRATION: 0.000 Hrs
 FERRY : 0.628 Hrs

 TOTAL HOURS: 5.500 Hrs

 BACKED by Matt Trevenen on 30/10/2000

JOB : 1455.4
 CLIENT : CAMECO
 AREA : Alligator River
 FLIGHT : 008
 JULIAN : 285
 DATE : 0/2000
 AIRCRAFT: VH-WGS

 ON LINE : 472.7 kms 1.626 Hrs
 SCRUB : 0.0 kms 0.000 Hrs
 OVERFLY : -61.5 kms
 PRODUCTION : 411.2 kms 1.626 Hrs
 TURN AROUND: 1.056 Hrs
 CALIBRATION: 0.000 Hrs
 FERRY : 2.318 Hrs

 TOTAL HOURS: 5.000 Hrs

APPENDIX III – Flight Summary

BELOW IS A LISTING OF ALL TRAVERSE AND TIE LINES.

Line	Flight	Date	Start fiducial	End fiducial	Start time	End time
40010	4	20001006	241.0	610.9	08:45:40.0	08:51:49.9
40020	4	20001006	611.0	986.9	08:53:54.0	09:00:09.9
40030	4	20001006	987.0	1382.9	09:02:08.0	09:08:43.9
40040	4	20001006	1383.0	1747.9	09:10:37.0	09:16:41.9
40050	4	20001006	1748.0	2141.9	09:18:44.0	09:25:17.9
40060	4	20001006	2142.0	2507.9	09:27:54.0	09:33:59.9
40070	4	20001006	2508.0	2903.9	09:35:58.0	09:42:33.9
40080	4	20001006	2904.0	3272.9	09:44:39.0	09:50:47.9
40090	4	20001006	3273.0	3672.9	09:52:40.0	09:59:19.9
40100	4	20001006	3673.0	4040.9	10:01:34.0	10:07:41.9
40110	4	20001006	4041.0	4429.9	10:09:11.0	10:15:39.9
40120	4	20001006	4430.0	4805.9	10:17:25.0	10:23:40.9
40130	4	20001006	4806.0	5198.9	10:25:17.0	10:31:49.9
40140	4	20001006	5199.0	5571.9	10:33:26.0	10:39:38.9
40150	4	20001006	5572.0	5964.9	10:41:17.0	10:47:49.9
40160	4	20001006	5965.0	6331.9	10:49:31.0	10:55:37.9
40170	4	20001006	6332.0	6719.9	10:57:11.0	11:03:38.9
40180	4	20001006	6720.0	7084.9	11:05:39.0	11:11:43.9
40190	4	20001006	7085.0	7464.9	11:14:00.0	11:20:19.9
40200	4	20001006	7465.0	7832.9	11:22:35.0	11:28:42.9
40210	4	20001006	7833.0	8213.9	11:30:38.0	11:36:58.9
40220	4	20001006	8214.0	8581.9	11:39:07.0	11:45:14.9
40230	4	20001006	8582.0	8978.9	11:47:45.0	11:54:21.9
40240	4	20001006	8979.0	9356.9	11:56:24.0	12:02:41.9
40250	4	20001006	9357.0	9726.9	12:04:32.0	12:10:41.9
40260	4	20001006	9727.0	10101.9	12:12:36.0	12:18:50.9
40270	4	20001006	10102.0	10478.9	12:20:32.0	12:26:48.9
40280	4	20001006	10479.0	10854.9	12:28:32.0	12:34:47.9
40290	4	20001006	10855.0	11233.9	12:36:38.0	12:42:56.9
40291	6	20001009	241.0	610.9	08:22:59.0	08:29:08.9
40300	4	20001006	11234.0	11608.9	12:44:47.0	12:51:01.9
40301	6	20001009	611.0	1007.9	08:31:26.0	08:38:02.9
40310	6	20001009	1008.0	1410.9	08:39:47.0	08:46:29.9
40320	6	20001009	1411.0	1797.9	08:48:31.0	08:54:57.9
40330	6	20001009	1798.0	2169.9	08:56:51.0	09:03:02.9
40340	6	20001009	2170.0	2551.9	09:04:47.0	09:11:08.9
40350	6	20001009	2552.0	2930.9	09:12:47.0	09:19:05.9
40360	6	20001009	2931.0	3315.9	09:20:53.0	09:27:17.9
40370	6	20001009	3316.0	3694.9	09:29:12.0	09:35:30.9
40380	6	20001009	3695.0	4076.9	09:37:28.0	09:43:49.9
40390	6	20001009	4077.0	4461.9	09:45:13.0	09:51:37.9
40400	6	20001009	4462.0	4840.9	09:53:17.0	09:59:35.9
40410	6	20001009	4841.0	5222.9	10:01:22.0	10:07:43.9
40420	6	20001009	5223.0	5604.9	10:09:41.0	10:16:02.9
40430	6	20001009	5605.0	5986.9	10:17:46.0	10:24:07.9
40440	6	20001009	5987.0	6367.9	10:25:58.0	10:32:18.9
40450	6	20001009	6368.0	6744.9	10:34:13.0	10:40:29.9
40460	6	20001009	6745.0	7119.9	10:42:15.0	10:48:29.9
40470	6	20001009	7120.0	7493.9	10:50:23.0	10:56:36.9
40480	6	20001009	7494.0	7875.9	10:58:19.0	11:04:40.9

Line	Flight	Date	Start fiducial	End fiducial	Start time	End time
------	--------	------	----------------	--------------	------------	----------

40490	6	20001009	7876.0	8254.9	11:06:29.0	11:12:47.9
40500	6	20001009	8255.0	8630.9	11:14:45.0	11:21:00.9
40510	6	20001009	8631.0	9008.9	11:22:41.0	11:28:58.9
40520	6	20001009	9009.0	9379.9	11:31:50.0	11:38:00.9
40530	6	20001009	9380.0	9745.9	11:39:48.0	11:45:53.9
40540	6	20001009	9746.0	10122.9	11:47:47.0	11:54:03.9
40550	6	20001009	10123.0	10523.9	11:55:50.0	12:02:30.9
40560	6	20001009	10524.0	10904.9	12:04:30.0	12:10:50.9
40570	6	20001009	10905.0	11278.9	12:12:26.0	12:18:39.9
40580	6	20001009	11279.0	11658.9	12:20:17.0	12:26:36.9
40590	6	20001009	11659.0	12027.9	12:28:17.0	12:34:25.9
40600	6	20001009	12028.0	12408.9	12:36:01.0	12:42:21.9
40610	6	20001009	12409.0	12773.9	12:44:21.0	12:50:25.9
40620	6	20001009	12774.0	13164.9	12:52:07.0	12:58:37.9
40630	6	20001009	13165.0	13565.9	13:00:19.0	13:06:59.9
40631	8	20001011	1.0	359.9	11:11:52.0	11:17:50.9
40632	8	20001011	1552.0	1914.9	11:58:14.0	12:04:16.9
40640	6	20001009	13566.0	13972.9	13:08:32.0	13:15:18.9
40641	8	20001011	360.0	746.9	11:19:21.0	11:25:47.9
40642	8	20001011	1915.0	2280.9	12:06:04.0	12:12:09.9
40650	8	20001011	747.0	1109.9	11:27:30.0	11:33:32.9
40651	8	20001011	2281.0	2660.9	12:13:42.0	12:20:01.9
47010	8	20001011	1110.0	1216.9	11:38:27.0	11:40:13.9
47011	8	20001011	2661.0	2778.9	12:22:10.0	12:24:07.9
47020	8	20001011	1217.0	1337.9	11:41:37.0	11:43:37.9
47021	8	20001011	2779.0	2896.9	12:25:29.0	12:27:26.9
47030	8	20001011	1338.0	1440.9	11:44:50.0	11:46:32.9
47031	8	20001011	2897.0	3002.9	12:28:37.0	12:30:22.9
47040	8	20001011	1441.0	1551.9	11:47:55.0	11:49:45.9
47041	8	20001011	3003.0	3122.9	12:31:34.0	12:33:33.9
47050	8	20001011	3123.0	3235.9	12:34:46.0	12:36:38.9
47060	8	20001011	3236.0	3353.9	12:37:39.0	12:39:36.9
47070	8	20001011	3354.0	3458.9	12:40:43.0	12:42:27.9
47080	8	20001011	3459.0	3580.9	12:43:31.0	12:45:32.9
47090	8	20001011	3581.0	3681.9	12:46:41.0	12:48:21.9
47100	8	20001011	3682.0	3797.9	12:49:38.0	12:51:33.9
47110	8	20001011	3798.0	3899.9	12:52:53.0	12:54:34.9
47120	8	20001011	3900.0	4016.9	12:55:56.0	12:57:52.9
47130	8	20001011	4017.0	4122.9	12:59:24.0	13:01:09.9
47140	8	20001011	4123.0	4250.9	13:02:30.0	13:04:37.9
47150	8	20001011	4251.0	4333.9	13:05:46.0	13:07:08.9
47151	8	20001011	4334.0	4434.9	13:09:47.0	13:11:27.9
47160	8	20001011	4435.0	4565.9	13:12:33.0	13:14:43.9
47170	8	20001011	4566.0	4666.9	13:15:47.0	13:17:27.9
47180	8	20001011	4667.0	4788.9	13:18:31.0	13:20:32.9
47190	8	20001011	4789.0	4888.9	13:21:50.0	13:23:29.9
47200	8	20001011	4889.0	5003.9	13:24:38.0	13:26:32.9
47210	8	20001011	5004.0	5102.9	13:27:44.0	13:29:22.9
47220	8	20001011	5103.0	5220.9	13:30:21.0	13:32:18.9
47230	8	20001011	5221.0	5324.9	13:33:26.0	13:35:09.9
47240	8	20001011	5325.0	5439.9	13:36:31.0	13:38:25.9
47250	8	20001011	5440.0	5540.9	13:39:27.0	13:41:07.9
47261	8	20001011	5541.0	5666.9	13:44:34.0	13:46:39.9
47270	8	20001011	5667.0	5769.9	13:47:53.0	13:49:35.9
47280	8	20001011	5770.0	5893.9	13:50:44.0	13:52:47.9

APPENDIX IV – List Of All Supplied Data

Documentation on GIS Data Package

All data on the accompanying CD is separated into folders based on type, area and source:

A1 HOME DIRECTORY

liverpool.apr - ESRI Arcview project file for viewing via Arcview Version 3.1 or better.

lp_*.aep - ESRI ArcExplorer project files. One for each view contained in liverpool.apr

agrs	-	gamma ray spectrometry
bgi	-	background information
bpr	-	background remote sensing
dtm	-	digital terrain model
mag	-	magnetics
swir	-	OARS short-wave infrared data
tir	-	TIPS thermal infrared data
vnir	-	visible near infrared data
vswir	-	vis/swir data i.e. entire OARS range

Software - ArcExplorer is supplied on this CD in folder "software". See *.pdf for installation and instructions. This free software or a more recent version is also available from the ESRI website (www.esri.com). Fugro Airborne Surveys provides no support for this software.

A2 FILE STRUCTURE

Cameco_Exploration - Data supplied by Cameco

Images - Raster data (generally tiff/tfw), sub-divided into:

District_Scale_Imagery	- this survey
Published_Maps	- government sourced
Regional_Scale_Imagery	- data from regional surveys plus Landsat scenes

Plotfiles_Layouts - various tiffs/jpegs used in report.

Shpfiles - vector data generated during interpretation, and sourced from elsewhere e.g. Cameco, NTDME. Sub-divided into folders based on data source. Folders contain shape files and Arcview Legend files (*.avl). Shape files are associated with avl's via similar name.

A3 AEROMAGNETICS NAMING CONVENTION

Files are named using the general conventions indicated below for magnetics, gamma-ray spectrometry and topographic data:

tmi	- total magnetic intensity
rtp	- reduced to pole total magnetic intensity
dtm	- digital terrain model
tot	- radiometric total count
pot	- radiometric potassium channel count
tho	- radiometric thorium channel count
ura	- radiometric uranium channel count
tern	- radiometric ternary image r,g,b = k,u,th
*_315	- example, illumination direction
*c	- colour image
*h	- greyscale image

A4 HYPERSPECTRAL PROFILING NAMING CONVENTION

oars_ls_compare - folder contains OARS and Landsat data, simulated Abrams ratio images for comparison.

lp_stdrtat/sr_* - standard ratios from OARS data
 water - water ratio
 iron - iron ratio
 clay - clay ratio
 ndvi - normalised difference vegetation index
 ls4_3 - example, Landsat Band 4/3 ratio

lp_all_unmix_* - end member unmixed using the entire VNIR/ SWIR spectrum.

claysub_* - relative abundance , unmixed with particular attention to the "clay" region of the SWIR spectra.

claysub_rgb* - red/ green/ blue composite of the indicated end members.

lp_tips_* - end members or ratios derived from unmixing of thermal infrared data.

tips_*rgb* -red/ green/ blue composite of the indicated TIPS end members.

*g - greyscale version of unmixing result

*c8 - colour clipped version of unmixing result (8 bit)

A5 DESCRIPTION FOR .\LIVERPOOL.APR

Data compiled within Arcview project on June 11, 2001 9:19 AM (.liverpool.apm)

1) AG_DIGITAL_ELEVATION_MODEL_(DEM) - 7 themes in this View. Scale: 182491

Boundary.shp .\shpfiles\general\shpfiles\boundary.shp (polyline)
 50k_drainage.shp .\shpfiles\digital_elevation\shpfiles\50k_drainage.shp (polyline)
 5m_contour.shp .\shpfiles\digital_elevation\shpfiles\5m_contour.shp (polyline)*
 Lp_pan_dtm_45h.tif .\images\district_scale_imagery\digital_elevation\imagery\lp_pan_dtm_45h.tif (image)*
 Lp_pan_dtm_315h.tif .\images\district_scale_imagery\digital_elevation\imagery\lp_pan_dtm_315h.tif (image)*
 Lp_dtm_c_pan.tif .\images\district_scale_imagery\digital_elevation\imagery\lp_dtm_c_pan.tif (image)*
 Lp_dtm_315c.tif .\images\district_scale_imagery\digital_elevation\imagery\lp_dtm_315c.tif (image)

2) AG_GAMMARAY_SPECTROMETRY - 23 themes in this View. Scale: 183075

Interp_sat_l.shp .\shpfiles\remote_sensing\landsat_tm\shpfiles\interp_sat_l.shp (polyline)
 Interp_sat_p.shp .\shpfiles\remote_sensing\landsat_tm\shpfiles\interp_sat_p.shp (polygon)*
 Lp_tc_315c.tif .\images\district_scale_imagery\gamma_ray_spectrometry\imagery\total_count\lp_tc_315c.tif (image)*
 Lp_ura_315c.tif .\images\district_scale_imagery\gamma_ray_spectrometry\imagery\uranium\lp_ura_315c.tif (image)*
 Lp_tho_315c.tif .\images\district_scale_imagery\gamma_ray_spectrometry\imagery\thorium\lp_tho_315c.tif (image)*
 Lp_pot_315c.tif .\images\district_scale_imagery\gamma_ray_spectrometry\imagery\potassium\lp_pot_315c.tif (image)*
 Lp_tern_step2.tif .\images\district_scale_imagery\gamma_ray_spectrometry\imagery\ternary\lp_tern_step2.tif (image)*
 Lp_tern_step.tif .\images\district_scale_imagery\gamma_ray_spectrometry\imagery\ternary\lp_tern_step.tif (image)*
 Lp_tern_pan_dtm_45c.tif .\images\district_scale_imagery\gamma_ray_spectrometry\imagery\ternary\lp_tern_pan_dtm_45c.tif (image)*
 Lp_tern_l.tif .\images\district_scale_imagery\gamma_ray_spectrometry\imagery\ternary\lp_tern_l.tif (image)
 Lp_tern_c_pan.tif .\images\district_scale_imagery\gamma_ray_spectrometry\imagery\ternary\lp_tern_c_pan.tif (image)*
 Lp_tern_c.tif .\images\district_scale_imagery\gamma_ray_spectrometry\imagery\ternary\lp_tern_c.tif (image)*
 Lp_pot_tho_ratio_l.tif .\images\district_scale_imagery\gamma_ray_spectrometry\imagery\ratios\lp_pot_tho_ratio_l.tif (image)*
 Lp_konu_l.tif .\images\district_scale_imagery\gamma_ray_spectrometry\imagery\ratios\lp_konu_l.tif (image)*
 Lp_uonk_l.tif .\images\district_scale_imagery\gamma_ray_spectrometry\imagery\ratios\lp_uonk_l.tif (image)*
 Lp_thonu_l.tif .\images\district_scale_imagery\gamma_ray_spectrometry\imagery\ratios\lp_thonu_l.tif (image)*
 Lp_uonth_l.tif .\images\district_scale_imagery\gamma_ray_spectrometry\imagery\ratios\lp_uonth_l.tif (image)*
 Merge_tc_315c_lease.tif .\images\regional_scale_imagery\gamma_ray_spectrometry\imagery\merge_tc_315c_lease.tif (image)*

Merge_tern_cs_lease.tif
 .\images\regional_scale_imagery\gamma_ray_spectrometry\imagery\merge_tern_cs_lease.tif (image)*
 Merge_tern_c_lease.tif
 .\images\regional_scale_imagery\gamma_ray_spectrometry\imagery\merge_tern_c_lease.tif (image)*
 Merge_u_315c_lease.tif
 .\images\regional_scale_imagery\gamma_ray_spectrometry\imagery\merge_u_315c_lease.tif (image)*
 Merge_th_315c_lease.tif
 .\images\regional_scale_imagery\gamma_ray_spectrometry\imagery\merge_th_315c_lease.tif (image)*
 Merge_k_315c_lease.tif
 .\images\regional_scale_imagery\gamma_ray_spectrometry\imagery\merge_k_315c_lease.tif (image)*

3) AG_MAGNETICS - 20 themes in this View. Scale: 181746

Interp_mag_l.shp .\shpfiles\magnetics\shpfiles\interp_mag_l.shp (polyline)
 Interp_sat_p.shp .\shpfiles\remote_sensing\landsat_tm\shpfiles\interp_sat_p.shp (polygon)*
 Milingimbi_geolrc.tif .\images\published_maps\milingimbi_geolrc.tif (image)*
 Lp_tmi_f1vdh.tif .\images\district_scale_imagery\magnetics\imagery\lp_tmi_f1vdh.tif (image)*
 Lp_tmi_45c.tif .\images\district_scale_imagery\magnetics\imagery\lp_tmi_45c.tif (image)*
 Lp_tmi_315c.tif .\images\district_scale_imagery\magnetics\imagery\lp_tmi_315c.tif (image)*
 Lp_rtp_f1vdh.tif .\images\district_scale_imagery\magnetics\imagery\lp_rtp_f1vdh.tif (image)*
 Lp_rtp_agc7_h.tif .\images\district_scale_imagery\magnetics\imagery\lp_rtp_agc7_h.tif (image)*
 Lp_rtp_agc5_h.tif .\images\district_scale_imagery\magnetics\imagery\lp_rtp_agc5_h.tif (image)*
 Lp_rtp_agc3_h.tif .\images\district_scale_imagery\magnetics\imagery\lp_rtp_agc3_h.tif (image)*
 Lp_rtp_45vh.tif .\images\district_scale_imagery\magnetics\imagery\lp_rtp_45vh.tif (image)*
 Lp_rtp_45c.tif .\images\district_scale_imagery\magnetics\imagery\lp_rtp_45c.tif (image)*
 Lp_rtp_315vh.tif .\images\district_scale_imagery\magnetics\imagery\lp_rtp_315vh.tif (image)*
 Lp_rtp_315c.tif .\images\district_scale_imagery\magnetics\imagery\lp_rtp_315c.tif (image)*
 Lp_rtp_1vdh.tif .\images\district_scale_imagery\magnetics\imagery\lp_rtp_1vdh.tif (image)*
 Lp_rtp_1vdc.tif .\images\district_scale_imagery\magnetics\imagery\lp_rtp_1vdc.tif (image)*
 Merge_tmi_45c_lease.tif .\images\regional_scale_imagery\magnetics\imagery\merge_tmi_45c_lease.tif (image)*
 Merge_rtp_f1vdh_lease.tif .\images\regional_scale_imagery\magnetics\imagery\merge_rtp_f1vdh_lease.tif (image)*
 Merge_tmi_315c_lease.tif .\images\regional_scale_imagery\magnetics\imagery\merge_tmi_315c_lease.tif (image)*
 Merge_tmi_1vdh_lease.tif .\images\regional_scale_imagery\magnetics\imagery\merge_tmi_1vdh_lease.tif (image)*

4) BACKGROUND_INFORMATION - 14 themes in this View. Scale: 652382

Boundary.shp .\shpfiles\general\shpfiles\boundary.shp (polyline)
 C_maj_towns.shp .\shpfiles\published_maps\shpfiles\c_maj_towns.shp (point)
 C_z53_prospects_u_minloc.shp .\shpfiles\published_maps\shpfiles\c_z53_prospects_u_minloc.shp (point)
 C_z53_prospects_all.shp .\shpfiles\published_maps\shpfiles\c_z53_prospects_all.shp (point)
 C_z53_deposits_u.shp .\shpfiles\published_maps\shpfiles\c_z53_deposits_u.shp (point)
 C_very_min_towns.shp .\shpfiles\published_maps\shpfiles\c_very_min_towns.shp (point)*
 C_roads.shp .\shpfiles\published_maps\shpfiles\c_roads.shp (polyline)
 C_parks.shp .\shpfiles\published_maps\shpfiles\c_parks.shp (polygon)
 C_min_towns.shp .\shpfiles\published_maps\shpfiles\c_min_towns.shp (point)*
 C_drainage.shp .\shpfiles\published_maps\shpfiles\c_drainage.shp (polyline)
 C_pastural.shp .\shpfiles\published_maps\shpfiles\c_pastural.shp (polygon)*
 C_d5306_geol.shp .\shpfiles\published_maps\shpfiles\c_d5306_geol.shp (polygon)
 C_d5302_geol.shp .\shpfiles\published_maps\shpfiles\c_d5302_geol.shp (polygon)
 C_coas2.shp .\shpfiles\published_maps\shpfiles\c_coas2.shp (polygon)

5) BACKGROUND_REMOTE_SENSING - 16 themes in this View. Scale: 188194

Bound_liverpool.shp .\shpfiles\general\shpfiles\boundaries\bound_liverpool.shp (polygon)
 Interp_sat_l.shp .\shpfiles\remote_sensing\landsat_tm\shpfiles\interp_sat_l.shp (polyline)*
 Interp_sat_p.shp .\shpfiles\remote_sensing\landsat_tm\shpfiles\interp_sat_p.shp (polygon)*
 Lp_oars_abrams_almost8.tif
 .\images\district_scale_imagery\mineral_mapping\imagery\oars_ls_compare\lp_oars_abrams_almost8.tif
 (image)
 Lp_ls_abrams_almost.tif
 .\images\district_scale_imagery\mineral_mapping\imagery\oars_ls_compare\lp_ls_abrams_almost.tif
 (image)
 Milingimbi_geolrc.tif .\images\published_maps\milingimbi_geolrc.tif (image)*
 Spot_pan_sub.tif .\images\regional_scale_imagery\remote_sensing\landsat_tm\spot_pan_sub.tif (image)*
 Landsat_pc123.tif .\images\regional_scale_imagery\remote_sensing\landsat_tm\landsat_pc123.tif (image)*
 Landsat_ndvi.tif .\images\regional_scale_imagery\remote_sensing\landsat_tm\landsat_ndvi.tif (image)*
 Landsat_large2r.tif .\images\regional_scale_imagery\remote_sensing\landsat_tm\landsat_large2r.tif (image)*
 Landsat_iron_ratio.tif .\images\regional_scale_imagery\remote_sensing\landsat_tm\landsat_iron_ratio.tif
 (image)*
 Landsat_clay_ratio.tif .\images\regional_scale_imagery\remote_sensing\landsat_tm\landsat_clay_ratio.tif
 (image)*
 Landsat_b741_pan_sub8.tif
 .\images\regional_scale_imagery\remote_sensing\landsat_tm\landsat_b741_pan_sub8.tif (image)*
 Landsat_b741.tif .\images\regional_scale_imagery\remote_sensing\landsat_tm\landsat_b741.tif (image)

Landsat_b542.tif .\images\regional_scale_imagery\remote_sensing\landsat_tm\landsat_b542.tif (image)*
 Landsat_b431_pan_sub8.tif .\images\regional_scale_imagery\remote_sensing\landsat_tm\landsat_b431_pan_sub8.tif (image)*

6) HYP_SHORTWAVE_INFRARED_(SWIR) - 27 themes in this View. Scale: 183369

Boundary.shp .\shpfiles\general\shpfiles\boundary.shp (polyline)*
 Hotlink_claysub_01_05.shp .\shpfiles\general\shpfiles\hotlink_claysub_01_05.shp (polygon)
 Interp_sat_l.shp .\shpfiles\remote_sensing\landsat_tm\shpfiles\interp_sat_l.shp (polyline)*
 Interp_sat_p.shp .\shpfiles\remote_sensing\landsat_tm\shpfiles\interp_sat_p.shp (polygon)*
 Claysub_09c.tif .\images\district_scale_imagery\mineral_mapping\imagery\loars\claysub_09c.tif (image)
 Claysub_09g.tif .\images\district_scale_imagery\mineral_mapping\imagery\loars\claysub_09g.tif (image)
 Claysub_08g.tif .\images\district_scale_imagery\mineral_mapping\imagery\loars\claysub_08g.tif (image)*
 Claysub_08c.tif .\images\district_scale_imagery\mineral_mapping\imagery\loars\claysub_08c.tif (image)*
 Claysub_07g.tif .\images\district_scale_imagery\mineral_mapping\imagery\loars\claysub_07g.tif (image)*
 Claysub_07c.tif .\images\district_scale_imagery\mineral_mapping\imagery\loars\claysub_07c.tif (image)*
 Claysub_06g.tif .\images\district_scale_imagery\mineral_mapping\imagery\loars\claysub_06g.tif (image)*
 Claysub_06c.tif .\images\district_scale_imagery\mineral_mapping\imagery\loars\claysub_06c.tif (image)*
 Claysub_05g.tif .\images\district_scale_imagery\mineral_mapping\imagery\loars\claysub_05g.tif (image)*
 Claysub_05c.tif .\images\district_scale_imagery\mineral_mapping\imagery\loars\claysub_05c.tif (image)*
 Claysub_04g.tif .\images\district_scale_imagery\mineral_mapping\imagery\loars\claysub_04g.tif (image)*
 Claysub_04c.tif .\images\district_scale_imagery\mineral_mapping\imagery\loars\claysub_04c.tif (image)*
 Claysub_03g.tif .\images\district_scale_imagery\mineral_mapping\imagery\loars\claysub_03g.tif (image)*
 Claysub_03c.tif .\images\district_scale_imagery\mineral_mapping\imagery\loars\claysub_03c.tif (image)*
 Claysub_02g.tif .\images\district_scale_imagery\mineral_mapping\imagery\loars\claysub_02g.tif (image)*
 Claysub_02c.tif .\images\district_scale_imagery\mineral_mapping\imagery\loars\claysub_02c.tif (image)*
 Claysub_01g.tif .\images\district_scale_imagery\mineral_mapping\imagery\loars\claysub_01g.tif (image)*
 Claysub_01c.tif .\images\district_scale_imagery\mineral_mapping\imagery\loars\claysub_01c.tif (image)*
 5m_contour.shp .\shpfiles\digital_elevation\shpfiles\5m_contour.shp (polyline)*
 Lp_tern_c.tif .\images\district_scale_imagery\gamma_ray_spectrometry\imagery\ternary\lp_tern_c.tif (image)
 Lp_pan_dtm_315h.tif .\images\district_scale_imagery\digital_elevation\imagery\lp_pan_dtm_315h.tif (image)*
 Lp_rtp_1vdh.tif .\images\district_scale_imagery\magnetics\imagery\lp_rtp_1vdh.tif (image)*
 Milingimbi_geolrc.tif .\images\published_maps\milingimbi_geolrc.tif (image)*

7) HYP_THERMAL_INFRARED_(TIR) - 14 themes in this View. Scale: 181334

Boundary.shp .\shpfiles\general\shpfiles\boundary.shp (polyline)
 Interp_sat_l.shp .\shpfiles\remote_sensing\landsat_tm\shpfiles\interp_sat_l.shp (polyline)*
 Lp_tips_um02c8.tif .\images\district_scale_imagery\mineral_mapping\imagery\tips\lp_tips_um02c8.tif (image)*
 Lp_tips_um04c8.tif .\images\district_scale_imagery\mineral_mapping\imagery\tips\lp_tips_um04c8.tif (image)*
 Lp_tips_um08c8.tif .\images\district_scale_imagery\mineral_mapping\imagery\tips\lp_tips_um08c8.tif (image)*
 Lp_tips_um020408c8.tif .\images\district_scale_imagery\mineral_mapping\imagery\tips\lp_tips_um020408c8.tif (image)*
 Lp_tips_248_rgb.tif .\images\district_scale_imagery\mineral_mapping\imagery\tips\lp_tips_248_rgb.tif (image)
 Lp_tips_silrat_g.tif .\images\district_scale_imagery\mineral_mapping\imagery\tips\lp_tips_silrat_g.tif (image)*
 5m_contour.shp .\shpfiles\digital_elevation\shpfiles\5m_contour.shp (polyline)*
 Interp_sat_p.shp .\shpfiles\remote_sensing\landsat_tm\shpfiles\interp_sat_p.shp (polygon)*
 Lp_pan_dtm_315h.tif .\images\district_scale_imagery\digital_elevation\imagery\lp_pan_dtm_315h.tif (image)*
 Lp_tern_c.tif .\images\district_scale_imagery\gamma_ray_spectrometry\imagery\ternary\lp_tern_c.tif (image)*
 Lp_rtp_1vdh.tif .\images\district_scale_imagery\magnetics\imagery\lp_rtp_1vdh.tif (image)*
 Milingimbi_geolrc.tif .\images\published_maps\milingimbi_geolrc.tif (image)*

8) HYP_VISIBLE_NEAR_INFRARED_(VNIR) - 8 themes in this View. Scale: 184552

Boundary.shp .\shpfiles\general\shpfiles\boundary.shp (polyline)
 5m_contour.shp .\shpfiles\digital_elevation\shpfiles\5m_contour.shp (polyline)*
 Interp_sat_l.shp .\shpfiles\remote_sensing\landsat_tm\shpfiles\interp_sat_l.shp (polyline)*
 Interp_sat_p.shp .\shpfiles\remote_sensing\landsat_tm\shpfiles\interp_sat_p.shp (polygon)*
 Lp_pan_dtm_315h.tif .\images\district_scale_imagery\digital_elevation\imagery\lp_pan_dtm_315h.tif (image)
 Lp_tern_c.tif .\images\district_scale_imagery\gamma_ray_spectrometry\imagery\ternary\lp_tern_c.tif (image)*
 Lp_rtp_1vdh.tif .\images\district_scale_imagery\magnetics\imagery\lp_rtp_1vdh.tif (image)*
 Milingimbi_geolrc.tif .\images\published_maps\milingimbi_geolrc.tif (image)*

9) HYP_VNIR_TO_SWIR_(ALL) - 51 themes in this View. Scale: 182201

Boundary.shp .\shpfiles\general\shpfiles\boundary.shp (polyline)
 Interp_sat_l.shp .\shpfiles\remote_sensing\landsat_tm\shpfiles\interp_sat_l.shp (polyline)*
 Interp_sat_p.shp .\shpfiles\remote_sensing\landsat_tm\shpfiles\interp_sat_p.shp (polygon)*

Lp_all_unmix_13c8.tif (image)*	.\\images\\district_scale_imagery\\mineral_mapping\\imagery\\oars\\lp_all_unmix_13c8.tif
Lp_all_unmix_13g.tif (image)*	.\\images\\district_scale_imagery\\mineral_mapping\\imagery\\oars\\lp_all_unmix_13g.tif
Lp_all_unmix_12c8.tif (image)*	.\\images\\district_scale_imagery\\mineral_mapping\\imagery\\oars\\lp_all_unmix_12c8.tif
Lp_all_unmix_12g.tif (image)*	.\\images\\district_scale_imagery\\mineral_mapping\\imagery\\oars\\lp_all_unmix_12g.tif
Lp_all_unmix_11c8.tif (image)*	.\\images\\district_scale_imagery\\mineral_mapping\\imagery\\oars\\lp_all_unmix_11c8.tif
Lp_all_unmix_11g.tif (image)*	.\\images\\district_scale_imagery\\mineral_mapping\\imagery\\oars\\lp_all_unmix_11g.tif
Lp_all_unmix_10c8.tif (image)*	.\\images\\district_scale_imagery\\mineral_mapping\\imagery\\oars\\lp_all_unmix_10c8.tif
Lp_all_unmix_10g.tif (image)*	.\\images\\district_scale_imagery\\mineral_mapping\\imagery\\oars\\lp_all_unmix_10g.tif
Lp_all_unmix_09c8.tif (image)*	.\\images\\district_scale_imagery\\mineral_mapping\\imagery\\oars\\lp_all_unmix_09c8.tif
Lp_all_unmix_09g.tif (image)*	.\\images\\district_scale_imagery\\mineral_mapping\\imagery\\oars\\lp_all_unmix_09g.tif
Lp_all_unmix_08c8.tif (image)*	.\\images\\district_scale_imagery\\mineral_mapping\\imagery\\oars\\lp_all_unmix_08c8.tif
Lp_all_unmix_08g.tif (image)*	.\\images\\district_scale_imagery\\mineral_mapping\\imagery\\oars\\lp_all_unmix_08g.tif
Lp_all_unmix_07c8.tif (image)*	.\\images\\district_scale_imagery\\mineral_mapping\\imagery\\oars\\lp_all_unmix_07c8.tif
Lp_all_unmix_07g.tif (image)*	.\\images\\district_scale_imagery\\mineral_mapping\\imagery\\oars\\lp_all_unmix_07g.tif
Lp_all_unmix_06c8.tif (image)*	.\\images\\district_scale_imagery\\mineral_mapping\\imagery\\oars\\lp_all_unmix_06c8.tif
Lp_all_unmix_06g.tif (image)*	.\\images\\district_scale_imagery\\mineral_mapping\\imagery\\oars\\lp_all_unmix_06g.tif
Lp_all_unmix_05c8.tif (image)*	.\\images\\district_scale_imagery\\mineral_mapping\\imagery\\oars\\lp_all_unmix_05c8.tif
Lp_all_unmix_05g.tif (image)*	.\\images\\district_scale_imagery\\mineral_mapping\\imagery\\oars\\lp_all_unmix_05g.tif
Lp_all_unmix_04c8.tif (image)*	.\\images\\district_scale_imagery\\mineral_mapping\\imagery\\oars\\lp_all_unmix_04c8.tif
Lp_all_unmix_04g.tif (image)*	.\\images\\district_scale_imagery\\mineral_mapping\\imagery\\oars\\lp_all_unmix_04g.tif
Lp_all_unmix_03c8.tif (image)*	.\\images\\district_scale_imagery\\mineral_mapping\\imagery\\oars\\lp_all_unmix_03c8.tif
Lp_all_unmix_03g.tif (image)*	.\\images\\district_scale_imagery\\mineral_mapping\\imagery\\oars\\lp_all_unmix_03g.tif
Lp_all_unmix_02c8.tif (image)*	.\\images\\district_scale_imagery\\mineral_mapping\\imagery\\oars\\lp_all_unmix_02c8.tif
Lp_all_unmix_02g.tif (image)*	.\\images\\district_scale_imagery\\mineral_mapping\\imagery\\oars\\lp_all_unmix_02g.tif
Lp_all_unmix_01c8.tif (image)*	.\\images\\district_scale_imagery\\mineral_mapping\\imagery\\oars\\lp_all_unmix_01c8.tif
Lp_all_unmix_01g.tif (image)*	.\\images\\district_scale_imagery\\mineral_mapping\\imagery\\oars\\lp_all_unmix_01g.tif
Lp_all_unmix_00c8.tif (image)	.\\images\\district_scale_imagery\\mineral_mapping\\imagery\\oars\\lp_all_unmix_00c8.tif
Lp_all_unmix_00g.tif (image)	.\\images\\district_scale_imagery\\mineral_mapping\\imagery\\oars\\lp_all_unmix_00g.tif
5m_contour.shp	.\\shpfiles\\digital_elevation\\shpfiles\\5m_contour.shp (polyline)*
Milingimbi_geolrc.tif	.\\images\\published_maps\\milingimbi_geolrc.tif (image)*
Lp_pan_dtm_315h.tif	.\\images\\district_scale_imagery\\digital_elevation\\imagery\\lp_pan_dtm_315h.tif (image)*
Lp_tern_c.tif (image)*	.\\images\\district_scale_imagery\\gamma_ray_spectrometry\\imagery\\ternary\\lp_tern_c.tif
Lp_stdtrat_iron.tif	.\\images\\district_scale_imagery\\mineral_mapping\\imagery\\oars\\lp_stdtrat_iron.tif (image)*
Lp_stdtrat_clay.tif	.\\images\\district_scale_imagery\\mineral_mapping\\imagery\\oars\\lp_stdtrat_clay.tif (image)*
Lp_stdtrat_dveg.tif	.\\images\\district_scale_imagery\\mineral_mapping\\imagery\\oars\\lp_stdtrat_dveg.tif (image)*
Lp_stdtrat_gveg.tif	.\\images\\district_scale_imagery\\mineral_mapping\\imagery\\oars\\lp_stdtrat_gveg.tif (image)*
Lp_stdtrat_ndvi.tif	.\\images\\district_scale_imagery\\mineral_mapping\\imagery\\oars\\lp_stdtrat_ndvi.tif (image)*
Lp_stdtrat_water.tif (image)*	.\\images\\district_scale_imagery\\mineral_mapping\\imagery\\oars\\lp_stdtrat_water.tif
Lp_sr06_ls7_5.tif	.\\images\\district_scale_imagery\\mineral_mapping\\imagery\\oars\\lp_sr06_ls7_5.tif (image)*

Lp_sr07_ls7_4.tif	.\\images\\district_scale_imagery\\mineral_mapping\\imagery\\oars\\lp_sr07_ls7_4.tif (image)*
Lp_sr08_ls5_7.tif	.\\images\\district_scale_imagery\\mineral_mapping\\imagery\\oars\\lp_sr08_ls5_7.tif (image)*
Lp_sr09_ls5_4.tif	.\\images\\district_scale_imagery\\mineral_mapping\\imagery\\oars\\lp_sr09_ls5_4.tif (image)*
Lp_sr10_ls5_1.tif	.\\images\\district_scale_imagery\\mineral_mapping\\imagery\\oars\\lp_sr10_ls5_1.tif (image)*
Lp_sr11_ls4_7.tif	.\\images\\district_scale_imagery\\mineral_mapping\\imagery\\oars\\lp_sr11_ls4_7.tif (image)*
Lp_sr12_ls4_3.tif	.\\images\\district_scale_imagery\\mineral_mapping\\imagery\\oars\\lp_sr12_ls4_3.tif (image)*
Lp_sr13_ls4_2.tif	.\\images\\district_scale_imagery\\mineral_mapping\\imagery\\oars\\lp_sr13_ls4_2.tif (image)*
Lp_sr14_ls3_2.tif	.\\images\\district_scale_imagery\\mineral_mapping\\imagery\\oars\\lp_sr14_ls3_2.tif (image)*
Lp_sr15_ls3_1.tif	.\\images\\district_scale_imagery\\mineral_mapping\\imagery\\oars\\lp_sr15_ls3_1.tif (image)*

A6 LAYOUTS - 7 TOTAL LAYOUTS

Figure_3_11, Scale: 100000
 Figure_3_12, Scale: 100000
 Figure_3_13, Scale: 100000
 Figure_3_14, Scale: 100000
 Figure_3_15, Scale: 100000
 Figure_3_16, Scale: 100000
 Figure_3_17, Scale: 100000

TABLES - 0 Total Tables
 This project contains no Tables

SCRIPTS - 0 Total Scripts
 This project contains no Scripts

CHARTS - 0 Total Charts
 This project contains no Charts

DIALOGS - 0 Total Dialogs
 This project contains no Dialogs

NOTES:

* Theme is not drawn in the view

^ Tables contains Joins

! View NOT Live Linked

ALL PATHS IN THIS PROJECT:

- .\\images\\district_scale_imagery\\digital_elevation\\imagery
- .\\images\\district_scale_imagery\\gamma_ray_spectrometry\\imagery\\potassium
- .\\images\\district_scale_imagery\\gamma_ray_spectrometry\\imagery\\ratios
- .\\images\\district_scale_imagery\\gamma_ray_spectrometry\\imagery\\ternary
- .\\images\\district_scale_imagery\\gamma_ray_spectrometry\\imagery\\thorium
- .\\images\\district_scale_imagery\\gamma_ray_spectrometry\\imagery\\total_count
- .\\images\\district_scale_imagery\\gamma_ray_spectrometry\\imagery\\uranium
- .\\images\\district_scale_imagery\\magnetics\\imagery
- .\\images\\district_scale_imagery\\mineral_mapping\\imagery\\oars
- .\\images\\district_scale_imagery\\mineral_mapping\\imagery\\oars_ls_compare
- .\\images\\district_scale_imagery\\mineral_mapping\\imagery\\tips
- .\\images\\published_maps
- .\\images\\regional_scale_imagery\\gamma_ray_spectrometry\\imagery
- .\\images\\regional_scale_imagery\\magnetics\\imagery
- .\\images\\regional_scale_imagery\\remote_sensing\\landsat_tm
- .\\shpfiles\\digital_elevation\\shpfiles
- .\\shpfiles\\general\\shpfiles
- .\\shpfiles\\general\\shpfiles\\boundaries
- .\\shpfiles\\magnetics\\shpfiles
- .\\shpfiles\\published_maps\\shpfiles
- .\\shpfiles\\remote_sensing\\landsat_tm\\shpfiles

GRIDS – IN ERMAPPER FORMAT

Total magnetic Intensity
Total Count
Potassium
Uranium
Thorium
ADT

Verification flight path plot in HPGL format @ 1:50,000